Journal of Sound and Vibration 494 (2021) 115858

Contents lists available at ScienceDirect

Journal of Sound and Vibration

journal homepage: www.elsevier.com/locate/jsv

Active control of linear vibrating systems for antiresonance assignment with regional pole placement

Dario Richiedei*, Iacopo Tamellin

Department of Management and Engineering, University of Padova, Italy

ARTICLE INFO

Article history:
Received 21 March 2020
Revised 8 November 2020
Accepted 18 November 2020
Available online 23 November 2020

Keywords:
Vibrating systems
Antiresonance assignment
Regional pole placement
Active control
Linear matrix inequality

ABSTRACT

This paper proposes a novel method for antiresonance assignment and regional pole placement in linear time-invariant vibrating systems, by means of state feedback control. The method also handles asymmetric systems and unstable ones too. Additionally, it works with both point and cross-receptances and handles the simultaneous assignment of more antiresonances in the same receptance.

The method relies on two stages. In the first stage, the desired pairs of closed-loop zeros of a prescribed receptance are exactly assigned. In the second stage, all the closed-loop system poles are placed within the desired region of the complex plane. This feature allows the controller to impose the system stability and to feature the desired dynamic properties through a regional pole placement. Since the gain correction computed in the second stage is obtained as a solution of the homogeneous system related to the zero-assignment problem, it does not cause any spillover on the assigned zeros. The first step exploits the receptance method for gain computing, while the second step uses the first-order model formulation to exploit all the benefits of the Linear Matrix Inequality theory, by formulating a bilinear matrix problem solved as a semidefinite optimization aimed at reducing the control effort.

The chief original contribution of the proposed method is that it embeds an a-priori imposition of both the closed-loop stability and the pole clustering in the desired regions, by overcoming the limitations of most of the methods appeared in the literature. The method effectiveness is demonstrated through five meaningful test cases.

1. Introduction

1.1. Motivations and general introduction

Antiresonance assignment, often denoted as zero assignment, is a powerful technique for vibration control since it allows local vibration absorption by imposing one or more antiresonances (i.e. a pair of complex conjugate zeros) in the receptance from the force exciting the c-th degree of freedom (DOF) to the displacement of the r-th coordinate. In such a way, when the system is excited at the c-th DOF by a harmonic force matching the antiresonance frequency, the steady state vibration at the r-th coordinate vanishes.

* Corresponding author. Stradella S. Nicola 3, 36100 Vicenza, Italy.
E-mail addresses: dario.richiedei@unipd.it (D. Richiedei), iacopo.tamellin@phd.unipd.it (I. Tamellin).

https://doi.org/10.1016/j.jsv.2020.115858
0022-460X/

Passive and active approaches have been developed over the decades to cope with this task. The formers exploit the use of passive devices such as masses, inerters, dampers or springs, to modify the system inertial, damping and elastic properties, either by increasing the number of DOFs (see e.g. [1–3]) or by preserving it ([4–8]). In contrast, active control techniques ([9–14]) exploit active devices such as actuators that supply the desired control forces based on the measures provided by sensors and feed back to the controller. Semi-active approaches have been also developed, where active devices are adopted to adapt the antiresonance frequency ([15–17]).

The effect of the control can be thought of as an "active modification" of the system inertial, damping and elastic properties, although passive or active approaches are not equivalent in term of symmetry of the modifications. Indeed, in the case of passive approaches to antiresonance assignment, the additive modifications of the system matrices are symmetric and semi-definite positive, in accordance with the well-known reciprocity law. Hence, the modified system will preserve the symmetry and positive semidefiniteness of the original one, as well as its asymptotic stability. In contrast, if active control is adopted, the additive modifications of the open-loop system matrices are usually asymmetric, unless co-located control is performed. Hence, the closed-loop system matrices can become asymmetric and negative definite. Therefore, placing the system zeros by means of active control, can lead to system instability if the pole spillover is not properly accounted for in the controller design.

1.2. State of the art on zero assignment through active control

Antiresonance assignment through active control has been studied by the most eminent researchers in the field of dynamic structural modification, that have proposed some meaningful results for linear time-invariant (LTI) systems. One of the first works addressing active antiresonance assignment in vibrating systems has been proposed by Ram in [9], where the author proposed a state feedback method to assign the zeros of a receptance together with two poles, while the remaining poles match those of the open-loop system. The method computes the position feedback gain and the force distribution vector for the case of rank-one control, by admitting also sparse vectors, and has been developed with reference to symmetric, undamped systems, with no possibility of modifying damping of pole or zero and zeros.

A milestone in the field of active control of LTI vibrating systems is the work [10] proposed by Mottershead and Ram. This work introduces the receptance method to active vibration control and applies it to assign a set of zeros, as well as to concurrently assign a set of poles and zeros in the case of full state-feedback control of symmetric LTI systems. Such a method does not account for spillover on the unassigned poles due to zero assignment, and hence does not ensure the asymptotic stability of the controlled system for any arbitrary system and set of desired zeros. The risk of instability has been overcome in [11] where Mottershead et al. focused on assigning the zeros of a point-receptance, together with the poles in the case of co-located output feedback in symmetric LTI vibrating systems. Hence, stability is always ensured for negative feedback due to the pole-zero interlacing properties of co-located systems.

Active antiresonance assignment for symmetric LTI systems with time delay has been investigated by Singh et al. in [12] and [13], where the authors exploited the Taylor series in order to compute the control gains for the assignment of one pair of complex conjugate zeros of a receptance, in the case of single-input and single-output control. The limitation of this method is that it does not introduce any a-priori condition to ensure the asymptotic stability of the controlled system.

1.3. Contributions of this paper

The literature review highlights that the methods available in the literature are focused on the assignment of the zeros, while do not include any a-priori condition for the proper placement in the complex plane of the unassigned closed-loop poles. In the light of this limitation, the goal of this paper is to include specifications on all the closed-loop poles to ensure stability and to ensure the desired transient properties such as damping, settling time, decay rate. This is here achieved by clustering the poles in some suitable sub-regions of the left-hand half-plane. This approach is denoted as "regional pole placement" by contrast with usual pole placement that is pointwise and requires each pole to lie in an exact point of the complex plane. Relaxing the specification on the poles allows for imposing the antiresonances while clustering all the poles.

A two-stage strategy is adopted. In the first stage, pointwise assignment of the desired pairs of zeros is done in the receptance of interest, by solving an underdetermined linear system formulated by means of the receptance approach proposed in [10]. The degrees of freedom in the solution of such a system of linear equations are then exploited in the second stage to cluster all the poles in the region of interest, while avoiding spillover on the assigned zeros. In the second stage, the theory of Linear Matrix Inequality (LMI) is adopted.

The convenience of exploiting two-stage approaches in vibration control has been already shown in the field of pole placement (see e.g. [18,19]) In the less-investigated case of antiresonance assignment, it is enforced by the fact that the methods based on just the first-order models of the system are usually not suitable for several reasons. First, they usually require the inversion of the mass matrix of the adjunct system which can be ill-conditioned or even singular (as often happens for cross-receptances). Additionally, the adjunct system is often nearly uncontrollable. In the light of these limitations, ad-hoc methods have been developed for antiresonance assignment in vibrating systems, as those exploited in the first stage of the proposed paper, although these methods have the limitations discussed in Section 1.2.

As for the use of the LMI theory, several papers have already successfully exploited it in the field of pole assignment. Indeed, it has been widely proved that LMI is effective in accomplishing other secondary tasks for the control, besides place-

ment of the poles; additionally, LMIs can be solved numerically through well-established and reliable numerical optimization algorithms. A common secondary task of LMIs is enhancing the closed-loop system robustness by assuming different structures of the uncertainties (see e.g. [20–24]). Indeed, with some conservatism, the robust assignment of the closed-loop poles can be solved through LMI optimization [20]. Robust pole placement of linear systems using state-derivative feedback has been also solved through LMI in [25]. Mixed H_2/H_∞ control synthesis with regional pole placement is also solved through LMI in [20]. Constraints on the size of feedback gain can be catered naturally through LMI, to find the minimum feedback gain with respect to different norms, to perform pole placement [26]. The use of LMI regions to prescribe the system transient dynamics has been also successfully applied to partial eigenvalue assignment, by also exploiting left-eigenvectors parametrization [27]. LMIs have been attractive for the analysis of stability of systems affected by time delays too [28]. For example, in [18] the formulation of LMI regions for retarded systems are exploited to ensure stability of the secondary poles due to the time delay.

The literature review, summarized through the aforementioned papers, shows the great attention gained by pole placement in the control community; on the other hand, it reveals the lacks in the field of antiresonance assignment and the need to new methods to solve this relevant control problem.

The paper proposes the technique with its mathematical background (Section 2), and its validation by means of five different numerical test cases (Section 3). The examples are developed for the case of rank-one control, although the idea can be extended to higher-rank control with just some minor adaptations.

2. Method description

2.1. Problem statement

Let us consider a N-DOF LTI vibrating system modelled through its mass, damping, stiffness and input matrices, denoted respectively $\mathbf{M},\mathbf{C},\mathbf{K} \in \mathbb{R}^{N\times N}$, $\mathbf{b} \in \mathbb{R}^{N\times N_b}$ (N_b is the number of independent control forces). The displacement vector is $\mathbf{q} \in \mathbb{R}^N$, while the control forces are collected in vector $\mathbf{u} \in \mathbb{R}^{N_b}$. It is assumed that the system is controllable and that the full state feedback is available. The control forces are computed through the feedback gain matrices $\mathbf{f}$, $\mathbf{g} \in \mathbb{R}^{N\times N_b}$, to be computed to assign the desired dynamic behavior to the controlled system. The model of the controlled system in the time domain t is therefore:

$$\begin{cases} \mathbf{M}\ddot{\mathbf{q}}(t) + \mathbf{C}\dot{\mathbf{q}}(t) + \mathbf{K}\mathbf{q}(t) = \mathbf{b}\mathbf{u}(t) \\ \mathbf{u}(t) = -\mathbf{f}^{\mathbf{T}}\dot{\mathbf{q}}(t) - \mathbf{g}^{\mathbf{T}}\mathbf{q}(t) \end{cases} \tag{1}$$

The poles of the system are the roots of the characteristic equation $P_p(s)$:

$$P_p(s) = \det\left(s^2\mathbf{M} + s\mathbf{C} + \mathbf{K}\right) \tag{2}$$

The zeros of the receptance $h_{rc}(s)$, from the force exciting the c-th DOF to the displacement of the r-th DOF, are the roots of the characteristic equation $P_z^{rc}(s)$:

$$P_z^{rc}(s) = \det\left(s^2\mathbf{M_{rc}} + s\mathbf{C_{rc}} + \mathbf{K_{rc}}\right) \tag{3}$$

Matrices $\mathbf{M_{rc}}, \mathbf{C_{rc}}, \mathbf{K_{rc}} \in \mathbb{R}^{(N-1)\times(N-1)}$ are obtained by removing the r-th column and the c-th row from the original system matrices $\mathbf{M}, \mathbf{C}, \mathbf{K} \in \mathbb{R}^{N\times N}$ and lead to the so-called adjunct system.

Given a self-conjugate set of $N_z \leq 2(N-1)$ zeros, $\mu_1, ..., \mu_{N_z} \in \mathbb{C}$, the aim of the control design is to compute the feedback gains such that N_z closed-loop zeros are exactly assigned for an arbitrary receptance $h_{rc}(s)$ (from the c-th force to the response of the r-th coordinate) while the poles $\lambda_1, ..., \lambda_{2N} \in \mathbb{C}$ preserve asymptotic stability by lying in the left half of the complex plane or in some prescribed locations of the stable half-plane. Two problems can be therefore stated and will be solved within the same mathematical frame. In all the problems, the system matrices $\mathbf{M}$, $\mathbf{C}$, $\mathbf{K}$, $\mathbf{b}$ are assumed as fixed and known.

Problem 1. Given a receptance $h_{rc}(s)$ and a self-conjugate set of $N_z \leq 2(N-1)$ desired zeros $\sum_d = \{\mu_1, \mu_2, ..., \mu_{N_z}\}$, finding the gain matrices $\mathbf{f}$ and $\mathbf{g}$ such that:

1 The closed-loop system receptance $h_{rc}(s)$ has the desired zeros;
2 The set of the closed-loop system poles $\{\lambda_1, \lambda_2, ..., \lambda_{2N}\}$ ensures asymptotic stability, i.e. $\mathrm{Re}(\lambda) < 0$ for any λ.

Problem 2. Given a receptance $h_{rc}(s)$ and a self-conjugate set of $N_z \leq 2(N-1)$ desired zeros $\sum_d = \{\mu_1, \mu_2, ..., \mu_{N_z}\}$, finding the gain matrices $\mathbf{f}$ and $\mathbf{g}$ such that:

1 The closed-loop system receptance $h_{rc}(s)$ has the desired zeros;
2 The closed-loop poles $\{\lambda_1, \lambda_2, ..., \lambda_{2N}\}$ lies in a prescribed subregion of the complex plane, denoted D.

The solving strategy proposed in this paper for the two problems is a two stages approach. In the first stage, the gains ensuring the correct placement of the desired zeros are computed by exploiting and adapting some reliable methods proposed in the literature, such as those using the system receptances. In the second stage, by exploiting the no-spillover condition on such zeros and LMI constraints, the poles are assigned in accordance with the requirement of each problem.

2.2. Formulation of the closed-loop zero assignment problem

The placement of the N_z desired closed-loop zeros $\mu_1, \mu_2, ..., \mu_{N_z}$ can be performed by any of the methods proposed in the literature, whenever it is numerically reliable. An effective way is exploiting the receptance matrix of the system. Indeed, although the method proposed in this paper will require the system matrices in the second stage, the use of receptance in the zero-assignment stage is convenient to handle possible numerical ill conditionings. For example, the well-established receptance method proposed in [10] is here adopted, and briefly recalled in this Section, to handle the case of rank-one control, i.e. $N_b = 1$. Nonetheless, the idea proposed in this work can be extended to an arbitrary number of control inputs, by adopting proper methods for solving the zero-assignment problem in the first stage, or just through a recursive application of the first stage of the proposed method [29].

In the case of rank-one control, the receptance matrix of the open-loop, $\mathbf{H}(s)$, and closed-loop $\tilde{\mathbf{H}}(s)$ systems are defined as:

$$\mathbf{H}(s) = \left(s^2\mathbf{M} + s\mathbf{C} + \mathbf{K}\right)^{-1} \in \mathbb{C}^{N\times N} \tag{4}$$

and

$$\tilde{\mathbf{H}}(s) = \left(s^2\mathbf{M} + s\left(\mathbf{C} + \mathbf{b}\mathbf{f}^{\mathbf{T}}\right) + \left(\mathbf{K} + \mathbf{b}\mathbf{g}^{\mathbf{T}}\right)\right)^{-1} \in \mathbb{C}^{N\times N} \tag{5}$$

The rc-th term in the receptance matrix of the closed-loop system can be computed by exploiting the Sherman-Morrison formula and some algebraic manipulations:

$$\tilde{h}_{rc}(s) = \frac{\mathbf{e}_\mathbf{r}^{\mathbf{T}}\left[\left(1 + (s\mathbf{f} + \mathbf{g})^{\mathbf{T}}\mathbf{H}(s)\mathbf{b}\right)\mathbf{H}(s) - \mathbf{H}(s)\mathbf{b}(s\mathbf{f} + \mathbf{g})^{\mathbf{T}}\mathbf{H}(s)\right]\mathbf{e}_\mathbf{c}}{1 + (s\mathbf{f} + \mathbf{g})^{\mathbf{T}}\mathbf{H}(s)\mathbf{b}} \tag{6}$$

where $\mathbf{e_r}$ and $\mathbf{e_c}$ are the unit vector obtained by extracting respectively the r-th and the c-th column from the identity matrix.

The zeros of the system are the roots of the numerator of Eq.(6). Therefore, for a desired zero μ_i, the control synthesis problem is finding the gains $\mathbf{f}$ and $\mathbf{g}$ ensuring that:

$$\mathbf{e}_\mathbf{r}^{\mathbf{T}}\left[\left(1 + (\mu_i\mathbf{f} + \mathbf{g})^{\mathbf{T}}\mathbf{H}(\mu_i)\mathbf{b}\right)\mathbf{H}(\mu_i) - \mathbf{H}(\mu_i)\mathbf{b}(\mu_i\mathbf{f} + \mathbf{g})^{\mathbf{T}}\mathbf{H}(\mu_i)\right]\mathbf{e}_\mathbf{c} = 0 \tag{7}$$

Once μ_i, $\mathbf{H}(\mu_i)$ and $\mathbf{b}$ are known, Eq.(7) is a linear problem in the unknown $\mathbf{f}$ and $\mathbf{g}$.

By defining the following auxiliary complex vector $\mathbf{t_i}$ as follows:

$$\mathbf{t_i} = h_{rc}(\mu_i)\mathbf{H}(\mu_i)\mathbf{b} - \left[\mathbf{e}_\mathbf{r}^{\mathbf{T}}\mathbf{H}(\mu_i)\mathbf{b}\right]\mathbf{H}(\mu_i)\mathbf{e_c} \tag{8}$$

and by collecting all the N_z assignment problems, it is possible to write the linear system for $i = 1, ..., N_z$ in matrix form:

$$\begin{bmatrix} \mu_1\mathbf{t}_1^{\mathbf{T}} & \mathbf{t}_1^{\mathbf{T}} \\ \mu_2\mathbf{t}_2^{\mathbf{T}} & \mathbf{t}_2^{\mathbf{T}} \\ \vdots & \vdots \\ \mu_{N_z}\mathbf{t}_{\mathbf{N_z}}^{\mathbf{T}} & \mathbf{t}_{\mathbf{N_z}}^{\mathbf{T}} \end{bmatrix} \begin{Bmatrix} \mathbf{f} \\ \mathbf{g} \end{Bmatrix} = \begin{Bmatrix} -h_{rc}(\mu_1) \\ -h_{rc}(\mu_2) \\ \vdots \\ -h_{rc}(\mu_{N_z}) \end{Bmatrix} \tag{9}$$

An extension for the case of asymmetric matrices is provided in Section 3.5.2.

2.3. Assignment of the desired closed-loop zeros

Eq.(9) reveals that the zero-assignment problem is a linear problem and each desired antiresonance frequency for one receptance leads to a pair of equations. The zero assignment condition can be therefore written in the compact notation of a linear system, with the obvious meaning of matrix $\mathbf{G} \in \mathbb{C}^{N_z\times 2N}$ and vector $\mathbf{y} \in \mathbb{C}^{N_z}$:

$$\mathbf{G}\mathbf{k} = \mathbf{y} \tag{10}$$

$\mathbf{k} = \begin{Bmatrix} \mathbf{f} \\ \mathbf{g} \end{Bmatrix} \in \mathbb{R}^{2N\times 1}$ is the gain vector for state feedback control.

Linear systems are also obtained for arbitrary rank and dimension of the input matrix $\mathbf{b}$.

Since the antiresonances are the roots of the characteristic equation of the adjoint system, their number is always smaller than N, and therefore the system Eq.(10) is underdetermined and has infinite solution. All these solutions lead to exactly fulfill the specifications on the zeros, while lead to different poles. Hence the computation of $\mathbf{k}$ should be performed carefully. A novel approach to tackle this problem is proposed in this paper.

To correctly solve the *Problems 1* and *2* the complete solution $\mathbf{k}$ of Eq.(10) should be chosen within a subspace of dimension $2N - N_z$ and defined as the sum of the particular solution of the non-homogeneous equation, denoted $\mathbf{k_0}$, and a solution $\mathbf{k_h}$ of the homogeneous system $\mathbf{G}\mathbf{k_h} = \mathbf{0}$:

$$\mathbf{k} = \mathbf{k_0} + \mathbf{k_h} \tag{11}$$

A more convenient way to formulate the solution of the homogeneous system is through the matrix $\mathbf{V}$ whose dimension is $2N \times (2N - N_z)$ and whose columns span the nullspace (kernel) of $\mathbf{G}$, i.e. $\mathbf{V} \in \text{span}(\ker(\mathbf{G}))$, and through vector which $\mathbf{k_r}$ represents a $(2N - N_z)$-dimensional vector of coefficients:

$$\mathbf{k} = \mathbf{k_0} + \mathbf{V}\mathbf{k_r} \tag{12}$$

Since $\sum_d$ is closed under conjugation, then matrix $\mathbf{V}$ can be conveniently chosen to be real, thus leading to a real vector $\mathbf{k_r}$.

Eq. (12) allows outlining the proposed method:

1. In the first stage, it is computed $\mathbf{k_0}$ to correctly place the desired pair of zeros. The pointwise pre-allocation of some poles can be also exploited in this stage to find a convenient solution that improves the numerical solution of the second stage or increase the robustness of the closed-loop system. The description of this stage is provided in Section 2.4.
2. In the second stage, it is computed $\mathbf{k_h}$ to place the poles. Since $\mathbf{k_h}$ is a solution of the homogeneous system related to the zero-assignment problem, $\mathbf{k_h}$ will not cause any spillover on the assigned zeros. On the other hand, it can correctly place the poles if properly computed. Details of the second stage are provided in Section 2.5.

2.4. First stage: assignment of the zeros

The particular solution $\mathbf{k_0}$ can be computed in several ways since the system in Eq.(10) will be always underdetermined. As a matter of fact, $\mathbf{G} \in \mathbb{C}^{N_z \times 2N}$ with $N_z \leq 2(N-1)$.

The easiest way is to solve the linear system by looking for the minimum norm solution, which is an effective approach to reduce the control effort. Since $\mathbf{k_0}$ should be real, the system in Eq. (10) can be transformed into the following one, to get a simpler numerical solution:

$$\begin{bmatrix} \text{Re}(\mathbf{G}) \\ \text{Im}(\mathbf{G}) \end{bmatrix} \mathbf{k_0} = \begin{bmatrix} \text{Re}(\mathbf{y}) \\ \text{Im}(\mathbf{y}) \end{bmatrix} \tag{13}$$

It should be noted that there will be only two linearly independent equations for each pair of complex conjugate desired zeros, and therefore Eq.(13) is still an underdetermined system.

An improved solution can be adopted if $N_z < 2(N-1)$, by temporarily placing $2N - N_z$ poles in some arbitrary locations ensuring that $\text{Re}(\lambda) < 0$, in the case of *Problem 1*, or belonging to the desired subregion D, that is a smaller region of the left-hand side complex plane, in the case of *Problem 2*. These poles will be perturbed by the term $\mathbf{k_h}$ in the second stage, still remaining in the desired subregion of the complex plane. The reason of this choice is selecting, among the infinite gain matrices placing the zeros, the one that fulfills the requirement on some poles too. Additionally, a wise choice of such poles is effective to increase the robustness of the closed-loop system too, as will be shown in the example in Section 3.4.

The system for the concurrent pole-zero assignment can be formulated, again, as an underdetermined or determined linear system, depending on the number of assigned poles and zeros:

$$\begin{bmatrix} \mathbf{G_z} \\ \mathbf{G_p} \end{bmatrix} \mathbf{k_0} = \begin{Bmatrix} \mathbf{y_z} \\ \mathbf{y_p} \end{Bmatrix} \tag{14}$$

where $\mathbf{G_p}\mathbf{k_0} = \mathbf{y_p}$ represents the undetermined linear system for the assignment of $2N - N_z$ poles. The formulation of $\mathbf{G_p}$ and $\mathbf{y_p}$ can be, for example, obtained through the already mentioned receptance method [10] and are here omitted in this paper for brevity.

2.5. Second stage: assignment of the poles within the desired feasible region

2.5.1. Definitions and preliminaries

Differently to the first stage of the method that can rely on receptances, this stage adopts the first-order realization of the dynamic model, to take advantage of the well-established mathematical frame of the LMIs.

By assuming that $\mathbf{M}$ is invertible, the system model in Eq.(1) can be cast in the first-order form:

$$\dot{\mathbf{x}}(t) = \mathbf{A}\mathbf{x}(t) + \mathbf{B}\mathbf{u}(t) \tag{15}$$

The state vector is $\mathbf{x} \in \mathbb{R}^{2N}$, $\mathbf{A} \in \mathbb{R}^{2N \times 2N}$ is the state transition matrix and $\mathbf{B} \in \mathbb{R}^{2N \times N_b}$ is the input matrix:

$$\mathbf{x} = \begin{Bmatrix} \dot{\mathbf{q}} \\ \mathbf{q} \end{Bmatrix} \quad \mathbf{A} = \begin{bmatrix} -\mathbf{M}^{-1}\mathbf{C} & -\mathbf{M}^{-1}\mathbf{K} \\ \mathbf{I} & \mathbf{0} \end{bmatrix} \quad \mathbf{B} = \begin{bmatrix} \mathbf{M}^{-1}\mathbf{b} \\ \mathbf{0} \end{bmatrix} \tag{16}$$

If $\mathbf{M}$ is not invertible, a similar problem formulation could be adopted by exploiting the descriptor-form of the first-order representation, and the suitable LMIs. This topic is, however, out of the scope of this paper.

The pole specifications of both *Problems 1* and *2* can be tackled by defining a subregion of the complex plane, henceforth denoted D, where the poles should lie. A first-order dynamical system $\dot{\mathbf{x}} = \mathbf{A}\mathbf{x}$ is called D-stable if all the eigenvalues of $\mathbf{A}$,

i.e. the system poles, belong to D. A simple characterization of the D-stability can be obtained through the LMI regions. An LMI region is characterized by the characteristic matrix $\boldsymbol{\Psi}_D(\mathbf{A}, \mathbf{X})$:

$$\boldsymbol{\Psi}_D(\mathbf{A}, \mathbf{X}) = \mathbf{R} \otimes \mathbf{X} + \mathbf{Z} \otimes (\mathbf{AX}) + \mathbf{Z}^{\mathbf{T}} \otimes (\mathbf{AX})^{\mathbf{T}} \tag{17}$$

where $\otimes$ denotes the Kronecker product, $\mathbf{R}$ is a symmetric matrix and $\mathbf{Z}$ is a matrix that are used to define the subset of the complex plane $D \subseteq \mathbb{C}$ as $D = \{c \in \mathbb{C} : \quad f_D(c) \prec 0\}$ and $f_D(c) = \mathbf{R} + c\mathbf{Z} + \bar{c}\mathbf{Z}^T$. LMI regions are convex and symmetric with respect to the real axis. For instance, the left-half plane is an LMI region obtained by setting $\boldsymbol{R} = 0$ and $\boldsymbol{Z} = 1$. LMI regions with different shapes such as conic sectors, vertical half-planes, horizontal strips, disks, ellipses, parabolas and hyperbolic sectors can obtained too by adopting suitable values of $\mathbf{R}$ and $\mathbf{Z}$ [20]. Section 3.2 provides some examples of LMI with the related definitions of $\mathbf{R}$ and $\mathbf{Z}$. Robustness of the solution can be also handled by LMI theory, by modifying $\boldsymbol{\Psi}_D$ to include stability conditions under uncertainty, such as those proposed in [21] or [30]. LMIs can be intersected too, to generate manifold LMI regions. Indeed, given two LMI regions D_1 and D_2, together with their characteristic matrices $\boldsymbol{\Psi}_{D_1}(\mathbf{A}, \mathbf{X})$ and $\boldsymbol{\Psi}_{D_2}(\mathbf{A}, \mathbf{X})$, the intersection $D = D_1 \cap D_2$ is an LMI region too, whose characteristic matrix is $\boldsymbol{\Psi}_{D_1 \cap D_2}(\mathbf{A}, \mathbf{X}) = \mathrm{diag}(\boldsymbol{\Psi}_{D_1}(\mathbf{A}, \mathbf{X}), \boldsymbol{\Psi}_{D_2}(\mathbf{A}, \mathbf{X}))$. Therefore, by exploiting LMIs it is possible to represent several regions of the complex plane ensuring the desired damping, overshoot, natural frequencies, rise time or settling time [20].

Given D, the system $\dot{\mathbf{x}} = \mathbf{Ax}$ is D-stable if and only if there exists a symmetric matrix $\mathbf{X}$ such that [20]:

$$\boldsymbol{\Psi}_D(\mathbf{A}, \mathbf{X}) \prec 0, \quad \mathbf{X} = \mathbf{X}^{\mathbf{T}} \succ 0 \tag{18}$$

2.5.2. Application of LMI regions to the placement of the closed-loop poles

Once $\mathbf{k_0}$ has been computed such that a set of closed-loop zeros have been properly assigned, for the receptance of interest, the closed-loop poles can be clustered into LMI regions exploiting the degree of freedom in the choice of the solution $\mathbf{k}$ provided by the term $\mathbf{Vk_r}$ in Eq.(12). Indeed, the first order realization of the controlled system is:

$$\dot{\mathbf{x}} = \left(\mathbf{A} - \mathbf{B}(\mathbf{k_0} + \mathbf{Vk_r})^{\mathbf{T}}\right)\mathbf{x} \tag{19}$$

that can be written in the following form by introducing the dynamic matrix of the system after the first stage of the control synthesis, denoted $\mathbf{A_1} = \mathbf{A} - \mathbf{Bk_0^T}$:

$$\dot{\mathbf{x}} = \left(\mathbf{A_1} - \mathbf{Bk_r^T V^T}\right)\mathbf{x} \tag{20}$$

Matrix $\boldsymbol{\Psi}_D$ of the LMI in Eq.(18) is recast in this case as follows:

$$\boldsymbol{\Psi}_D(\mathbf{A_1}, \mathbf{k_r}, \mathbf{X}) = \mathbf{R} \otimes \mathbf{X} + \mathbf{Z} \otimes \left(\left(\mathbf{A_1} - \mathbf{Bk_r^T V^T}\right)\mathbf{X}\right) + \mathbf{Z}^{\mathbf{T}} \otimes \left(\left(\mathbf{A_1} - \mathbf{Bk_r^T V^T}\right)\mathbf{X}\right)^{\mathbf{T}} \tag{21}$$

Hence, to achieve D-stability, for an arbitrary definition of D, it is necessary to compute $\mathbf{k_r}$ and $\mathbf{X}$ such that:

$$\boldsymbol{\Psi}_D(\mathbf{A_1}, \mathbf{k_r}, \mathbf{X}) \prec 0, \quad \mathbf{X} = \mathbf{X}^{\mathbf{T}} \succ 0 \tag{22}$$

The assignment problem for the closed-loop poles can be solved through the non-linear SDP optimization in Eq.(23):

$$\begin{aligned} &\min \quad \|\mathbf{Vk_r}\|^2 \\ &\text{subj} \quad \boldsymbol{\Psi}_D(\mathbf{A_1}, \mathbf{k_r}, \mathbf{X}) \prec 0 \\ &\qquad \mathbf{X} = \mathbf{X}^{\mathbf{T}} \succ 0 \end{aligned} \tag{23}$$

Since both $\mathbf{k_r}$ and $\mathbf{X}$ are unknown, Eq.(23) is a bilinear matrix inequality (BMI). Solving BMIs is not always trivial since BMIs are non-linear and non-convex function. Solution methods for BMIs are currently subject of wide researches in the mathematical research community and several software for solving them are now available. A simpler solution approach, that fits with the case under investigation, is also proposed in this paper by recasting the nonlinear problem in Eq.(23) into a linear one to be solved within the frame of LMI. The numerical tests will exploit it and will compare its results with those provided by a commercial BMI solver.

2.5.3. Transformation of the BMI into a LMI

Let us introduce an auxiliary unknown vector $\mathbf{d} = \mathbf{Vk_r}$ and define $\mathbf{p} = \mathbf{Xd}$. After some manipulations, Eq.(21) becomes a LMI with respect to $\mathbf{p}$ and $\mathbf{X}$:

$$\boldsymbol{\Psi}_D(\mathbf{A_1}, \mathbf{p}, \mathbf{X}) = \mathbf{R} \otimes \mathbf{X} + \mathbf{Z} \otimes \left(\mathbf{A_1 X} - \mathbf{Bp^T}\right) + \mathbf{Z}^{\mathbf{T}} \otimes \left(\mathbf{A_1 X} - \mathbf{Bp^T}\right)^{\mathbf{T}} \tag{24}$$

The D-stability condition in Eq.(18) is translated into the following one, with $\mathbf{p}$ and $\mathbf{X}$ as the unknowns:

$$\boldsymbol{\Psi}_D(\mathbf{A_1}, \mathbf{p}, \mathbf{X}) \prec 0, \quad \mathbf{X} = \mathbf{X}^{\mathbf{T}} \succ 0 \tag{25}$$

The solution of the LMI in Eq.(25) can be handled with a convex semidefinite programming (SDP), that is easily solvable with interior-point techniques. In this work it is proposed to compute the gains by solving the following SDP minimization:

$$\begin{aligned} &\min \quad \|\mathbf{p}\|^2 \\ &\text{subj} \quad \boldsymbol{\Psi}_D(\mathbf{A_1}, \mathbf{p}, \mathbf{X}) \prec 0 \\ &\qquad \mathbf{X} = \mathbf{X}^{\mathbf{T}} \succ 0 \end{aligned} \tag{26}$$

Table 1
Summary of the five test cases.

Test case section	3.2	3.3	3.4	3.5	3.6
System matrices	**M, C, K** Symmetric	**M, C, K** Symmetric	**M, C** Symmetric **K** Asymmetric	**M, C, K** Symmetric	**M, C, K** Symmetric
Number of DOFs	3	5	6	4	13
Model of the system	LP	LP	FEM	LP	FEM and LP
Number of assigned μ_z	1 complex conjugate pair	2 complex conjugate pairs	1 complex conjugate pair	1 complex conjugate pair	3 complex conjugate pairs
Point/Cross-receptance	Cross-receptance	Point-receptance	Point-receptance	Cross-receptance	Cross-receptance
Particular solution $\mathbf{k_0}$	Underdetermined system: Assigns μ_z	Underdetermined system: Assigns μ_z	Underdetermined system: Assigns μ_z and some λ_p	Fully determined system: Assigns μ_z and some λ_p	Underdetermined system: Assigns μ_z
LMI constraint on the poles	Real part and minimum damping	Real part	Real part	Real part	Minimum damping

This choice of the objective function enables to reduce the control gains in some sense, since:

$$\|\mathbf{p}\|^2 = \|\mathbf{X}\mathbf{V}\mathbf{k_r}\|^2 = \|\mathbf{V}\mathbf{k_r}\|_{\mathbf{X}}^2 \tag{27}$$

To improve the numerical reliability of the solution of problem in Eq.(26), it is often useful to approximate the negative definiteness condition of $\mathbf{\Psi}_D(\mathbf{A_1}, \mathbf{p}, \mathbf{X})$ and the positive definiteness condition of $\mathbf{X}$ by means of two scalar values ε_1 and ε_2 that multiply identity matrices $\mathbf{I}$ (each one with its proper dimension). Hence, the optimization in Eq.(26) is recast as:

$$\begin{aligned} \min \quad & \|\mathbf{p}\|^2 \\ \text{subj} \quad & \mathbf{\Psi}_D(\mathbf{A_1}, \mathbf{p}, \mathbf{X}) \prec -\varepsilon_1 \mathbf{I} \\ & \mathbf{X} = \mathbf{X^T} \succ \varepsilon_2 \mathbf{I} \end{aligned} \tag{28}$$

The theoretical value of scalars ε_1 and ε_2 is 0. However, in practice they approach zero and should be slightly tuned depending on the numerical scaling of the system matrices, on the solver, on the accuracy parameters of the numerical solutions and of the CPU. Indeed, the solution of SDP problems is numerically cumbersome when non-strict inequalities should be tackled. For example, the widely adopted interior-point solvers return a warning if strict inequalities have been implemented and often an error message that stops the algorithm is returned. Therefore, to satisfy strict inequalities it is necessary to define and satisfy non-strict inequalities and sometimes to relax them.

2.5.4. Computation of $\mathbf{k_r}$

Once Eq. (28) is solved and the optimal value $\mathbf{X_{opt}}$, $\mathbf{p_{opt}}$ are computed, $\mathbf{k_r}$ should be computed. Two approaches are suggested in this work.

The variable change that morphs the BMI in Eq.(21) into the LMI in Eq.(24) is exploited to compute vector $\mathbf{k_r}$ as:

$$\mathbf{k_r} = \mathbf{U}\mathbf{X}_{\mathbf{opt}}^{-1}\mathbf{p_{opt}} \tag{29}$$

where matrix $\mathbf{U}$is the left pseudoinverse of $\mathbf{V}$, i.e. $\mathbf{UV} = \mathbf{I}$.

The second approach is numerical and is suitable whenever the ill-conditioned computation of the pseudoinverse makes $\mathbf{k_r}$ violate the LMI constraints. Following this second approach, $\mathbf{k_r}$ is computed by solving a norm minimization problem looking for $\mathbf{k_r}$ that ensures that $\mathbf{X_{opt}}\mathbf{V}\mathbf{k_r}$ is the closest to $\mathbf{p_{opt}}$, in the presence of the LMI constraint obtained by imposing $\mathbf{X_{opt}}$ in the BMI in Eq.(21):

$$\mathbf{\Psi}_{D,lin}(\mathbf{A_1}, \mathbf{k_r}) = \mathbf{R} \otimes \mathbf{X_{opt}} + \mathbf{Z} \otimes \left(\left(\mathbf{A_1} - \mathbf{B}\mathbf{k}_\mathbf{r}^\mathbf{T}\mathbf{V}^\mathbf{T}\right)\mathbf{X_{opt}}\right) + \mathbf{Z}^\mathbf{T} \otimes \left(\left(\mathbf{A_1} - \mathbf{B}\mathbf{k}_\mathbf{r}^\mathbf{T}\mathbf{V}^\mathbf{T}\right)\mathbf{X_{opt}}\right)^\mathbf{T} \tag{30}$$

The following formulation is finally suggested:

$$\begin{aligned} \min \quad & \left\| \mathbf{V}\mathbf{k_r} - \mathbf{X}_{\mathbf{opt}}^{-1}\mathbf{p_{opt}} \right\|^2 \\ \text{subj} \quad & \mathbf{\Psi}_{D,lin}(\mathbf{A_1}, \mathbf{k_r}) \prec -\varepsilon_3 \mathbf{I} \end{aligned} \tag{31}$$

Preconditioning techniques, as those widely developed in the literature on linear algebra [31], could be adopted to boost convergence. The parameter ε_3 is a small scalar that is adopted to define non-strict inequalities and to relax them if necessary.

3. Numerical results

3.1. General description and implementation details

Five numerical test cases with rank-one control, are proposed for validating the method, by adopting different systems, also taken from the recent literature, and different assignment requirements. Table 1 summarizes the features of the test cases (LP denotes lumped parameter models).

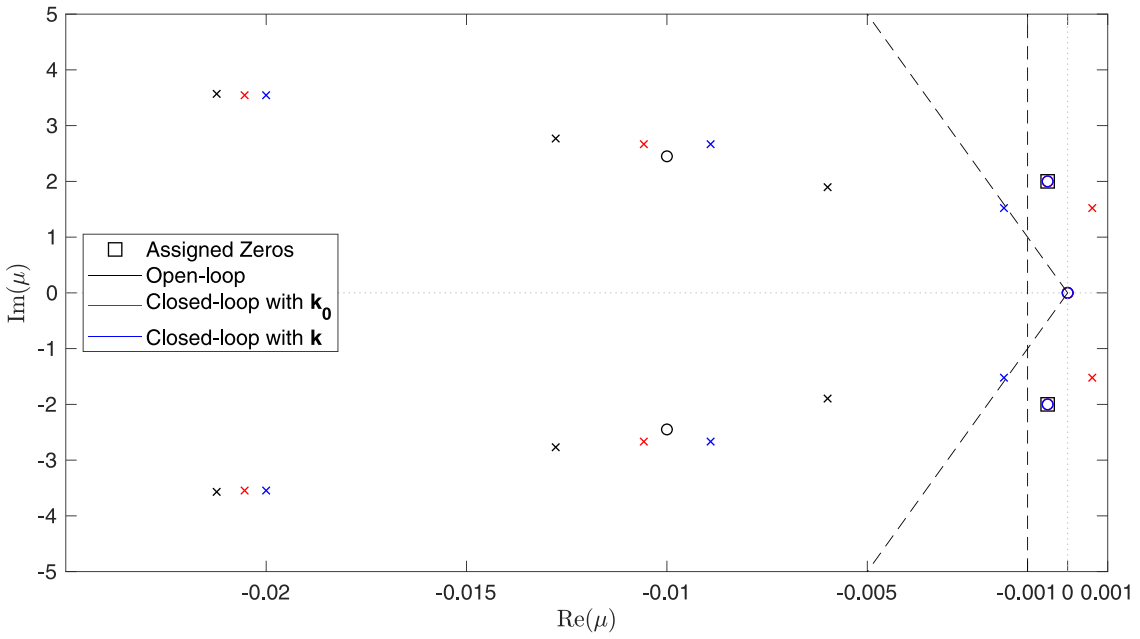

Fig. 1. Pole-zero map of $h_{32}(\mathrm{j}\omega)$ and $\tilde{h}_{32}(\mathrm{j}\omega)$ (test-case 1).

The least-square problem for the assignment of the zeros (see Eqs.(13) and (14)) have been solved exploiting the MATLAB *mldivide* function that effectively solves the underdetermined linear systems. The LMIs have been implement using the Yalmip interface for modeling optimization problems in MATLAB [32]. The linear SDP programming have been solved using the Mosek solver.

In the first test case, the outcomes of three different approaches for the computation of $\mathbf{k_r}$ are also shown: the linear SDP in Eq. (28) together with Eq. (29), the linear SDP in Eq. (28) together with the numerical method in Eq. (31), and the direct solution of the BMI in Eq. (23). In the latter case, The BMI optimization problem has been solved exploiting the PENLAB solver [33].

In the other test cases (Sections 3.3–3.6), only the results of the assignment obtained through the linear SDP in Eq.(28) together with Eq.(29) are reported, for brevity.

3.2. Case 1 – assignment of a pair of zero to a cross-receptance

The aim of this simple test case is to compare the results obtained by three different solution methods. The test case consists of a three-DOF lumped system whose matrices are:

$$\mathbf{M} = \mathrm{diag}(1,1,1) \quad \mathbf{C} = 0.01\begin{bmatrix} 2 & -1 & 0 \\ -1 & 3 & -1 \\ 0 & -1 & 3 \end{bmatrix} \quad \mathbf{K} = \begin{bmatrix} 6 & -3 & 0 \\ -3 & 9 & -3 \\ 0 & -3 & 9 \end{bmatrix} \quad \mathbf{b} = [1,\ 0,\ 0]^{\mathbf{T}} \tag{32}$$

The assignment task consists in assigning a pair of complex conjugate zeros of the cross-receptance $h_{32}(\mathrm{j}\omega)$ to $\mu_{1,2} = -0.0005 \pm j2$ while the closed-loop poles λ_i must belong to the region D defined as the intersection of two LMI regions D_1 and D_2:

- D_1 is a region in the left-half of the complex plane such that $\mathrm{Re}(\lambda_i) \leq -\sigma,\ i = 1, ..., 6$, with $\sigma = 0.001$. Matrix $\mathbf{\Psi}_{D1}$ in Eq.(24) is obtained by setting $\mathbf{R} = 2\sigma$ and $\mathbf{Z} = 1$ in Eq.(17):

$$\mathbf{\Psi}_{D_1}(\mathbf{A_1}, \mathbf{p}, \mathbf{X}) = \mathbf{A_1X} - \mathbf{Bp}^{\mathbf{T}} + \mathbf{XA}_{\mathbf{1}}^{\mathbf{T}} - \mathbf{pB}^{\mathbf{T}} + 2\sigma\mathbf{X} \prec 0 \tag{33}$$

- D_2 is a conic sector with magnitude 2θ such that the minimum damping of the poles is at least $\xi_{\min} = 0.001$, since $\xi = \cos(\theta)$. Matrix $\mathbf{\Psi}_{D2}$ is obtained by imposing $\mathbf{R} = \begin{bmatrix} 0 & 0 \\ 0 & 0 \end{bmatrix}$ and $\mathbf{Z} = \begin{bmatrix} \sin\theta & \cos\theta \\ -\cos\theta & \sin\theta \end{bmatrix}$:

$$\mathbf{\Psi}_{D_2}(\mathbf{A_1}, \mathbf{p}, \mathbf{X}) = \begin{bmatrix} \sin\theta\left(\mathbf{A_1X} - \mathbf{Bp}^{\mathbf{T}} + \mathbf{XA}_{\mathbf{1}}^{\mathbf{T}} - \mathbf{pB}^{\mathbf{T}}\right) & \cos\theta\left(\mathbf{A_1X} - \mathbf{Bp}^{\mathbf{T}} - \mathbf{XA}_{\mathbf{1}}^{\mathbf{T}} + \mathbf{pB}^{\mathbf{T}}\right) \\ \cos\theta\left(\mathbf{XA}_{\mathbf{1}}^{\mathbf{T}} - \mathbf{pB}^{\mathbf{T}} - \mathbf{A_1X} + \mathbf{Bp}^{\mathbf{T}}\right) & \sin\theta\left(\mathbf{A_1X} - \mathbf{Bp}^{\mathbf{T}} + \mathbf{XA}_{\mathbf{1}}^{\mathbf{T}} - \mathbf{pB}^{\mathbf{T}}\right) \end{bmatrix} \tag{34}$$

The LMI region bounds for both D_1 and D_2 are shown in Fig. 1 with a dashed line. The mathematical formulation of intersection of the two LMI regions is:

$$\mathbf{\Psi}_D(\mathbf{A_1}, \mathbf{p}, \mathbf{X}) = \mathrm{diag}(\mathbf{\Psi}_{D_1}(\mathbf{A_1}, \mathbf{p}, \mathbf{X}), \mathbf{\Psi}_{D_2}(\mathbf{A_1}, \mathbf{p}, \mathbf{X})) \tag{35}$$

Table 2
Gains (test-case 1).

Stage 1: $\mathbf{k_0}$	Stage 2: $\mathbf{k} = \mathbf{k_0} + \mathbf{V k_r}$						
		BMI Eq.(23)	LMI Eq.(28) and Eq.(29)	LMI Eq.(28) and Eq.(31)			
$\mathbf{f_0}$	$\mathbf{g_0}$	$\mathbf{f}$	$\mathbf{g}$	$\mathbf{f}$	$\mathbf{g}$	$\mathbf{f}$	$\mathbf{g}$
−0.0190	−2.0000	−0.0190	−2.0000	−0.0190	−2.0000	−0.0190	−2.0000
0.0000	0.0000	0.0087	0.0000	0.0091	0.0002	0.0043	0.0002
0.0000	0.0000	0.0039	0.0000	0.0040	0.0001	0.0012	0.0001

Table 3
Open-loop and closed-loop poles of the system, and zeros of $h_{32}(j\omega)$ and $\tilde{h}_{32}(j\omega)$, computed through Eq. (28) and Eq.(29) (test-case 1).

Open-loop zeros	Desired closed-loop zeros	Closed-loop zeros with $\mathbf{k_0}$	Closed-loop zeros with $\mathbf{k}$
$\mu_{1,2} = -0.01 \pm j2.45$	$\mu^d_{1,2} = -0.0005 \pm j2$	$\mu_{1,2} = -0.0005 \pm j2$	$\mu_{1,2} = -0.0005 \pm j2$
Open-loop poles	Desired closed-loop poles	Closed-loop poles with $\mathbf{k_0}$	Closed-loop poles with $\mathbf{k}$
$\lambda_{1,2} = -0.0060 \pm j1.90$	$\mathrm{Re}(\lambda_{1,2}) \leq -0.001$ $\xi(\lambda_{1,2}) \geq 0.001$	$\lambda_{1,2} = +0.0006 \pm j1.52$	$\lambda_{1,2} = -0.0016 \pm j1.52$
$\lambda_{3,4} = -0.0128 \pm j2.77$	$\mathrm{Re}(\lambda_{3,4}) \leq -0.001$ $\xi(\lambda_{3,4}) \geq 0.001$	$\lambda_{3,4} = -0.0106 \pm j2.67$	$\lambda_{3,4} = -0.0089 \pm j2.67$
$\lambda_{5,6} = -0.0212 \pm j3.57$	$\mathrm{Re}(\lambda_{5,6}) \leq -0.001$ $\xi(\lambda_{5,6}) \geq 0.001$	$\lambda_{5,6} = -0.0205 \pm j3.55$	$\lambda_{5,6} = -0.0200 \pm j3.55$

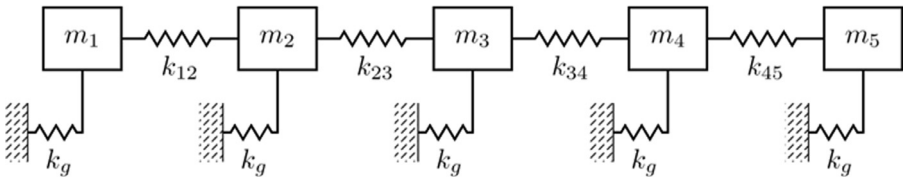

Fig. 2. Sketch of the five-mass system (test-case 2).

To provide evidence of the hazard of pole spillover, and hence of the relevance and effectiveness of the second stage, $\mathbf{k_0}$ has been computed as the minimum norm vector ensuring the achievement zeros, without taking care of any pole. The least-square solution of the zero assignment leads to the gains reported in Table 2, which cause an unstable pair of complex conjugate poles, as reported in Table 3.

The modification of such gains performed in the second stage, by exploiting the *D*-stability constraints, ensures the stabilization of the system.

The comparison of the gain vector computed through the three solution strategy of the second step is proposed in Table 2. It should be noted that, solving the non-linear SDP (BMI) in Eq.(23) leads to slightly different gains, compared to those obtained solving the linear SDP. Nonetheless, the prescribed closed-loop poles and zeros are obtained for all the tests (see Table 3, where the results obtained through Eq.(28) and Eq.(29) are proposed). The solution of the BMI optimization, through a 64bit PC equipped with an Intel® Core i7–6500U processor (2.50 GHz) and an 8 GB RAM took an average CPU time of 10.9 s. On the other hand, solving the linear SDP in Eq.(28), with $\varepsilon_1 = \varepsilon_2 = 1e{-}5$, which has led to better numerical conditioning in the SDP solution and faster convergence, the average CPU time is just 0.9 s. The computation of $\mathbf{k_r}$ through the SDP in Eq.(31) (with ε_3 equal to -1e–3) required an average CPU time equal to 0.7 s.

Regardless of the approach used to compute $\mathbf{k_r}$ the resulting gains enable to obtain a set of closed-loop poles that features the desired dynamic properties set through the poles (i.e. stability, damping and settling time), and the assigned zero. The pole-zero map for the closed-loop system controlled with the gains obtained through the linear SDP by means of Eqs.(28) and (29) is reported in Fig. 2 and corroborates this statement. The pole-zero map for the other two solution approaches are almost identical and omitted for brevity.

3.3. Case 2 – assignment of two pair of zeros to a point-receptance of a five-mass system

The second test case applies the method to a widely-used testbed (see e.g. [34,35]), which consists of five simply-connected masses, which are in turn connected to the frame through grounding springs. A sketch of the system is reported in Fig. 2. The actuation force distribution vector is here assumed to be $\mathbf{b} = [1,\ 0,\ 1,\ 0,\ 0]^{\mathbf{T}}$.

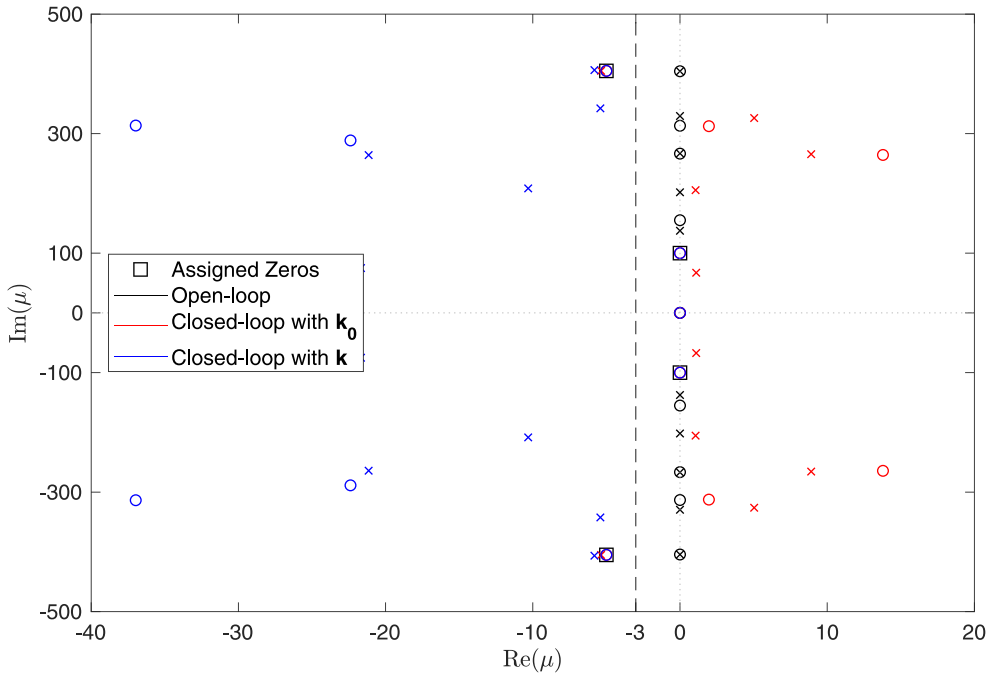

Fig. 3. Pole-zero map of $h_{22}(\mathrm{j}\omega)$ and $\tilde{h}_{22}(\mathrm{j}\omega)$ (test-case 2).

Table 4
Open-loop and closed-loop poles of the system, and zeros of $h_{22}(\mathrm{j}\omega)$ and $\tilde{h}_{22}(\mathrm{j}\omega)$ (test-case 2).

Open-loop zeros	Desired closed-loop zeros	Closed-loop zeros with $\mathbf{k_0}$	Closed-loop zeros with $\mathbf{k}$
$\mu_{1,2} = \pm\mathrm{j}155.1$	$\mu^d_{1,2} = \pm\mathrm{j}100$	$\mu_{1,2} = \pm\mathrm{j}100$	$\mu_{1,2} = \pm\mathrm{j}100$
$\mu_{3,4} = \pm\mathrm{j}404.4$	$\mu^d_{3,4} = -5 \pm \mathrm{j}405$	$\mu_{3,4} = -5 \pm \mathrm{j}405$	$\mu_{3,4} = -5 \pm \mathrm{j}405$
Open-loop poles	**Desired closed-loop poles**	**Closed-loop poles with $\mathbf{k_0}$**	**Closed-loop poles with $\mathbf{k}$**
$\lambda_{1,2} = \pm\mathrm{j}137.4$	$\mathrm{Re}(\lambda_{1,2}) \leq -3$	$\lambda_{1,2} = +1.1 \pm \mathrm{j}67.2$	$\lambda_{1,2} = -21.7 \pm \mathrm{j}75.0$
$\lambda_{3,4} = \pm\mathrm{j}201.9$	$\mathrm{Re}(\lambda_{3,4}) \leq -3$	$\lambda_{3,4} = +1.1 \pm \mathrm{j}205.4$	$\lambda_{3,4} = -10.3 \pm \mathrm{j}208.4$
$\lambda_{5,6} = \pm\mathrm{j}266.9$	$\mathrm{Re}(\lambda_{5,6}) \leq -3$	$\lambda_{5,6} = +8.9 \pm \mathrm{j}265.6$	$\lambda_{5,6} = -21.2 \pm \mathrm{j}264.1$
$\lambda_{7,8} = \pm\mathrm{j}329.5$	$\mathrm{Re}(\lambda_{7,8}) \leq -3$	$\lambda_{7,8} = +5.0 \pm \mathrm{j}326.1$	$\lambda_{7,8} = -5.4 \pm \mathrm{j}342.3$
$\lambda_{9,10} = \pm\mathrm{j}404.4$	$\mathrm{Re}(\lambda_{9,10}) \leq -3$	$\lambda_{9,10} = -5.4 \pm \mathrm{j}405.2$	$\lambda_{9,10} = -5.8 \pm \mathrm{j}406.4$

The system is undamped and its mass and stiffness matrices are:

$$\mathbf{M} = \mathrm{diag}(m_1, m_2, m_3, m_4, m_5)$$
$$\mathbf{K} = \begin{bmatrix} k_g + k_{12} & -k_{12} & 0 & 0 & 0 \\ -k_{12} & k_g + k_{12} + k_{23} & -k_{23} & 0 & 0 \\ 0 & -k_{23} & k_g + k_{23} + k_{34} & -k_{34} & 0 \\ 0 & 0 & -k_{34} & k_g + k_{34} + k_{45} & -k_{45} \\ 0 & 0 & 0 & -k_{45} & k_g + k_{45} \end{bmatrix} \tag{36}$$

The values of the parameters are: $m_1 = 1.727\,\mathrm{kg}$, $m_2 = 5.123\,\mathrm{kg}$, $m_3 = 8.214\,\mathrm{kg}$, $m_4 = 2.609\,\mathrm{kg}$, $m_5 = 1.339\,\mathrm{kg}$, $k_{12} = 75.14\,\mathrm{kNm^{-1}}$, $k_{23} = 67.74\,\mathrm{kNm^{-1}}$, $k_{34} = 75.47\,\mathrm{kNm^{-1}}$, $k_{45} = 83.40\,\mathrm{kNm^{-1}}$ and $k_g = 94.26\,\mathrm{kNm^{-1}}$.

The goal of the control design is to assign two pairs of complex conjugate zeros of the point-receptance $h_{22}(\mathrm{j}\omega)$ to $\mu_{1,2} = \pm j100$ and $\mu_{3,4} = -5 \pm j405$ while the closed-loop poles $\lambda_1, ..., \lambda_{10} \in \mathbb{C}$ must ensure that $\mathrm{Re}(\lambda_i) \leq -3$, $i = 1, ..., 10$. Computing the minimum norm solution of Eq.(13), by discarding any requirement on the poles, leads to the following gains: $\mathbf{f_0} = [-9.39, 0, -132.01, 0, 673.38]^\mathbf{T}$ and $\mathbf{g_0} = [0, 0, -1.25\mathrm{e}5, 0, 0]^\mathbf{T}$. The closed-loop system exactly features the desired zeros of $h_{22}(\mathrm{j}\omega)$, but is unstable since some poles lie on the right-half of the complex plane, as show in Fig. 3.

The solution of the semidefinite programming in Eq. (26) with the imposed LMI constraint, with $\varepsilon_1 = \varepsilon_2 = 1\mathrm{e}-8$, leads to the gains $\mathbf{f} = [79.5, 528.0, 679.1, -1623.7, -389.0]^\mathbf{T}$ and $\mathbf{g} = [2.55\mathrm{e}4, 0.19\mathrm{e}4, -7.75\mathrm{e}4, -2.06\mathrm{e}5, 7.89\mathrm{e}4]^\mathbf{T}$.

Fig. 3 and Table 4 reveal that all the control specifications are correctly fulfilled. As a further proof of the correct assignment, magnitude plots of $h_{22}(j\omega)$ before and after the modification are compared in Fig. 4.

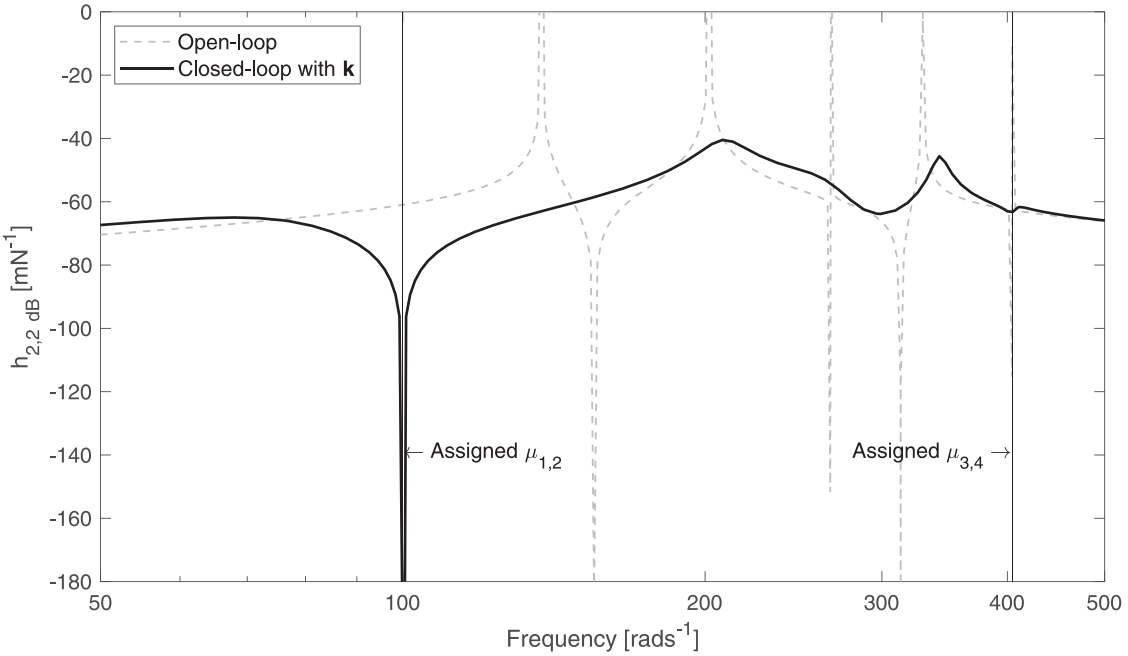

Fig. 4. Magnitude of $h_{22}(\mathrm{j}\omega)$ before and after the modification (test-case 2).

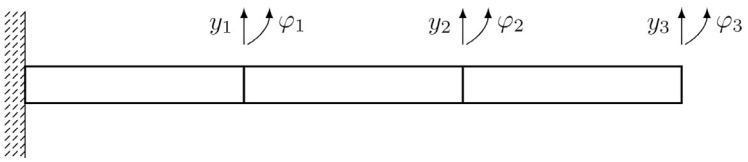

Fig. 5. Sketch of the cantilever beam (test-case 3).

3.4. Case 3 – assignment of a pair of zeros to a point-receptance of a cantilever beam

In the third test case, a continuous system modeled though finite elements is proposed. The system is a cantilever beam with rectangular cross-section area, modeled by means of three Euler-Bernoulli beams with equal lengths. The system is sketched in Fig. 5 and the following parameters have been adopted: Young modulus 70 GPa, mass density 2400 kgm^{-3}, area moment of inertia 2.13e − 10 m^4, transversal area 1.6e − 4 m^2. The system is undamped and is actuated by a single force that excites the translation of the first and the third node (DOFs number 1 and 5), leading to $\mathbf{b} = [1,\ 0,\ 0,\ 0,\ 1,\ 0]^{\mathbf{T}}$.

The system matrices have been scaled to improve the numerical conditioning of the problem, by means of two scalar scaling parameters γ and β. The scaled system matrices are therefore defined as:

$$\tilde{\mathbf{M}} = \beta^{-2}\gamma^{-1}\mathbf{M} \quad \tilde{\mathbf{K}} = \gamma^{-1}\mathbf{K} \tag{37}$$

The solution of the first stage of the proposed method should be performed by calculating the scaled system receptances as:

$$\tilde{\mathbf{H}}(j\tilde{\omega}) = \left(\tilde{\omega}^2\tilde{\mathbf{M}} + \tilde{\mathbf{K}}\right)^{-1} \text{ with } \tilde{\omega} = \beta\omega \tag{38}$$

The computed gains for the scaled system are therefore

$$\tilde{\mathbf{k}}_{\mathbf{0}} = \begin{bmatrix} \tilde{\mathbf{f}}_{\mathbf{0}} & \tilde{\mathbf{g}}_{\mathbf{0}} \end{bmatrix}^{\mathbf{T}} = \begin{bmatrix} \beta^{-1}\gamma^{-1}\mathbf{f_0} & \gamma^{-1}\mathbf{g_0} \end{bmatrix}^{\mathbf{T}} \tag{39}$$

which are then transformed to the gains of the unscaled system as follows:

$$\mathbf{f_0} = \beta\gamma\tilde{\mathbf{f}}_{\mathbf{0}},\ \mathbf{g_0} = \gamma\tilde{\mathbf{g}}_{\mathbf{0}}. \tag{40}$$

In the same way, the second stage of the method uses scaled state-space matrices.

The problem specification is to assign a pair of complex conjugate zeros of the point-receptance $h_{33}(\mathrm{j}\omega)$ to $\mu_{1,2} = -3 \pm$ j900, where the third DOF is the displacement y_2 of the cantilever beam, as shown in Fig. 5. Moreover, it is required that $\mathrm{Re}(\lambda_i) \leq -5,\ i = 1, ..., 12$. The following scaling parameters have been adopted: $\gamma = 1\mathrm{e}3$ and $\beta = 1\mathrm{e} - 4$.

In the solution of the first stage, two different pre-allocations of the closed-loop poles are compared to show the benefits in term of robustness. In the strategy denoted as “A”, three pairs of complex conjugate poles are temporarily assigned

Table 5
Gains (test-case 3).

Strategy A			
Stage 1: $\mathbf{k_{0,A}}$		Stage 2: $\mathbf{k_A} = \mathbf{k_{0,A}} + \mathbf{V k_{r,A}}$	
$\mathbf{f_{0,A}}$	$\mathbf{g_{0,A}}$	$\mathbf{f_A}$	$\mathbf{g_A}$
0.0000	0.00	−0.2369	−97.82
0.0977	700.38	0.0279	668.57
0.4061	−4682.40	1.0901	−4343.40
0.0434	2235.80	0.0002	2224.60
0.0000	0.00	−0.0405	−128.95
0.0586	−77.71	0.0806	−54.93
Strategy B			
Stage 1: $\mathbf{k_{0,B}}$		Stage 2: $\mathbf{k_B} = \mathbf{k_{0,B}} + \mathbf{V k_{r,B}}$	
$\mathbf{f_{0,B}}$	$\mathbf{g_{0,B}}$	$\mathbf{f_B}$	$\mathbf{g_B}$
12.9048	−352,630	10.5741	46,256
2.5810	−45,498	−0.0196	9083.40
−64.4526	−125,100	68.4822	−60,342
−0.6984	−89,955	0.7763	13,042
46.0460	58,048	39.2278	2760.40
−5.9006	−47,709	1.2130	8141.80

Table 6
Open-loop and closed-loop poles of the system, and zeros of $h_{33}(j\omega)$ and $\tilde{h}_{33}(j\omega)$ (test-case 3): with the pre-allocation strategy "A".

Open-loop zeros	Desired closed-loop zeros	Closed-loop zeros with $\mathbf{k_{0,A}}$	Closed-loop zeros with $\mathbf{k_A}$
$\mu_{1,2} = \pm$j436.8	$\mu^d_{1,2} = -3 \pm$ j900	$\mu_{1,2} = -3 \pm$ j900.0	$\mu_{1,2} = -3 \pm$ j900.0
Open-loop poles	Desired closed-loop poles	Closed-loop poles with $\mathbf{k_{0,A}}$	Closed-loop poles with $\mathbf{k_A}$
$\lambda_{1,2} = \pm$j89.5	$\mathrm{Re}(\lambda_{1,2}) \leq -5$	$\lambda_{1,2} = -5.0 \pm$ j300.0	$\lambda_{1,2} = -5.8 \pm$ j300.0
$\lambda_{3,4} = \pm$j562.6	$\mathrm{Re}(\lambda_{3,4}) \leq -5$	$\lambda_{3,4} = -5.0 \pm$ j700.0	$\lambda_{3,4} = -5.5 \pm$ j700.0
$\lambda_{5,6} = \pm$j1589.8	$\mathrm{Re}(\lambda_{5,6}) \leq -5$	$\lambda_{5,6} = -5.0 \pm$ j1500.0	$\lambda_{5,6} = -5.9 \pm$ j1501.3
$\lambda_{7,8} = \pm$j3580.2	$\mathrm{Re}(\lambda_{7,8}) \leq -5$	$\lambda_{7,8} = -23.3 \pm$ j3495.0	$\lambda_{7,8} = -24.0 \pm$ j3495.5
$\lambda_{9,10} = \pm$j6737.9	$\mathrm{Re}(\lambda_{9,10}) \leq -5$	$\lambda_{9,10} = +10.7 \pm$ j6633	$\lambda_{9,10} = -30.6 \pm$ j6637.0
$\lambda_{11,12} = \pm$j1.34e4	$\mathrm{Re}(\lambda_{11,12}) \leq -5$	$\lambda_{11,12} = -296 \pm$ j1.36e4	$\lambda_{11,12} = -296 \pm$ j1.36e4

to three sample locations within the LMI, whose real parts matches the bound of the LMI: $\lambda_{1,2} = -5.00 \pm$ j300.00, $\lambda_{3,4} = -5.00 \pm$ j700.00 and $\lambda_{5,6} = -5.00 \pm$ j1500.00. In the second strategy, denoted as "B", five complex conjugate poles are assigned within the LMI and far away from the imaginary axis, while their imaginary parts are is kept unchanged with respect to the open-loop: $\lambda_{1,2} = -100.00 \pm$ j89.50, $\lambda_{3,4} = -200.00 \pm 562.50$, $\lambda_{5,6} = -400.00 \pm$ j1589.80, $\lambda_{7,8} = -800.00 \pm$ j3580.20 and $\lambda_{9,10} = -1600.00 \pm$ j6737.90. This choice is expected to ensure higher robustness. After the first step (solved through Eq.(14) and leading to $\mathbf{k_{0,A}}$ and $\mathbf{k_{0,B}}$ displayed in Table 5), the closed-loop system features the poles and the zeros reported in Table 6. In both the cases, however, the controlled system is unstable since some of the unassigned poles have a positive real part. By applying the second step of the proposed method, all the real parts of the closed-loop poles become negative and lie within the LMI. Compared to those obtained through $\mathbf{k_{0,A}}$ and $\mathbf{k_{0,B}}$, all the poles have been modified to ensure *D*-stability, although they are still quite close to the pre-allocated locations. The gains that ensure the placement of the poles in the prescribed LMI region are reported in Table 5, and have been obtained by setting $\varepsilon_1 = \varepsilon_2 = 1\mathrm{e}-8$ in the solution of the SDP. The closed-loop system features the poles and the zeros reported in Tables 6 and 7 for strategy A and B respectively, the pole-zero map of $h_{33}(j\omega)$ is shown in Fig. 6 just for strategy A, for brevity of representation.

The positive effect on robustness of the pole pre-allocation in the first stage is here evaluated through the H-infinity norm of the transfer function $\mathbf{H_{ZW}}$ from the model uncertainty to the nominal state $\mathbf{x}$. By assuming the common structure of a state-multiplicative perturbation, $\mathbf{H_{ZW}}$ is defined through the following state space realization [19,36]:

$$\begin{bmatrix} \mathbf{A} - \mathbf{B}\mathbf{k}^{\mathbf{T}} & -\mathbf{B}\mathbf{k}^{\mathbf{T}} \\ \mathbf{I} & \mathbf{0} \end{bmatrix} \tag{41}$$

In accordance with the Small Gain Theorem, smaller values of $\|\mathbf{H_{ZW}}\|_\infty$ mean higher robustness with respect to the uncertainty. The application of such a theory to the example under investigation shows that Strategy B leads to higher robustness with respect to Strategy A. Fig. 7 corroborates this result, by comparing the maximum singular values for both the controllers and showing that $\max\{\bar{\sigma}(\mathbf{H_{ZW}}(\mathbf{k_A}))\} > \max\{\bar{\sigma}(\mathbf{H_{ZW}}(\mathbf{k_B}))\}$, as expected by the wise pre-allocation of the closed-loop poles in the first stage.

Table 7
Open-loop and closed-loop poles of the system, and zeros of $h_{33}(j\omega)$ and $\tilde{h}_{33}(j\omega)$ (test-case 3): with the pre-allocation strategy "B".

Open-loop zeros	Desired closed-loop zeros	Closed-loop zeros with $\mathbf{k_{0,B}}$	Closed-loop zeros with $\mathbf{k_B}$
$\mu_{1,2} = \pm$j436.8	$\mu^d_{1,2} = -3 \pm$ j900	$\mu_{1,2} = -3 \pm$ j900.0	$\mu_{1,2} = -3 \pm$ j900.0
Open-loop poles	**Desired closed-loop poles**	**Closed-loop poles with $\mathbf{k_{0,B}}$**	**Closed-loop poles with $\mathbf{k_B}$**
$\lambda_{1,2} = \pm$j89.5	$\mathrm{Re}(\lambda_{1,2}) \leq -5$	$\lambda_{1,2} = -100.0 \pm$ j89.5	$\lambda_{1,2} = -68.3 \pm$ j380.4
$\lambda_{3,4} = \pm$j562.6	$\mathrm{Re}(\lambda_{3,4}) \leq -5$	$\lambda_{3,4} = -200.0 \pm$ j562.5	$\lambda_{3,4} = -136.3 \pm$ j840.4
$\lambda_{5,6} = \pm$j1589.8	$\mathrm{Re}(\lambda_{5,6}) \leq -5$	$\lambda_{5,6} = -400 \pm$ j1589.8	$\lambda_{5,6} = -275.8 \pm$ j2638.2
$\lambda_{7,8} = \pm$j3580.2	$\mathrm{Re}(\lambda_{7,8}) \leq -5$	$\lambda_{7,8} = -800 \pm$ j3580.2	$\lambda_{7,8} = -559.1 \pm$ j4068.8
$\lambda_{9,10} = \pm$j6737.9	$\mathrm{Re}(\lambda_{9,10}) \leq -5$	$\lambda_{9,10} = -1600 \pm$ j6737.9	$\lambda_{9,10} = -1005 \pm$ j6608.7
$\lambda_{11,12} = \pm$j1.34e4	$\mathrm{Re}(\lambda_{11,12}) \leq -5$	$\lambda_{11} = -156.0$	$\lambda_{11,12} = -9053 \pm$ j10492
		$\lambda_{12} = 4.94$e4	

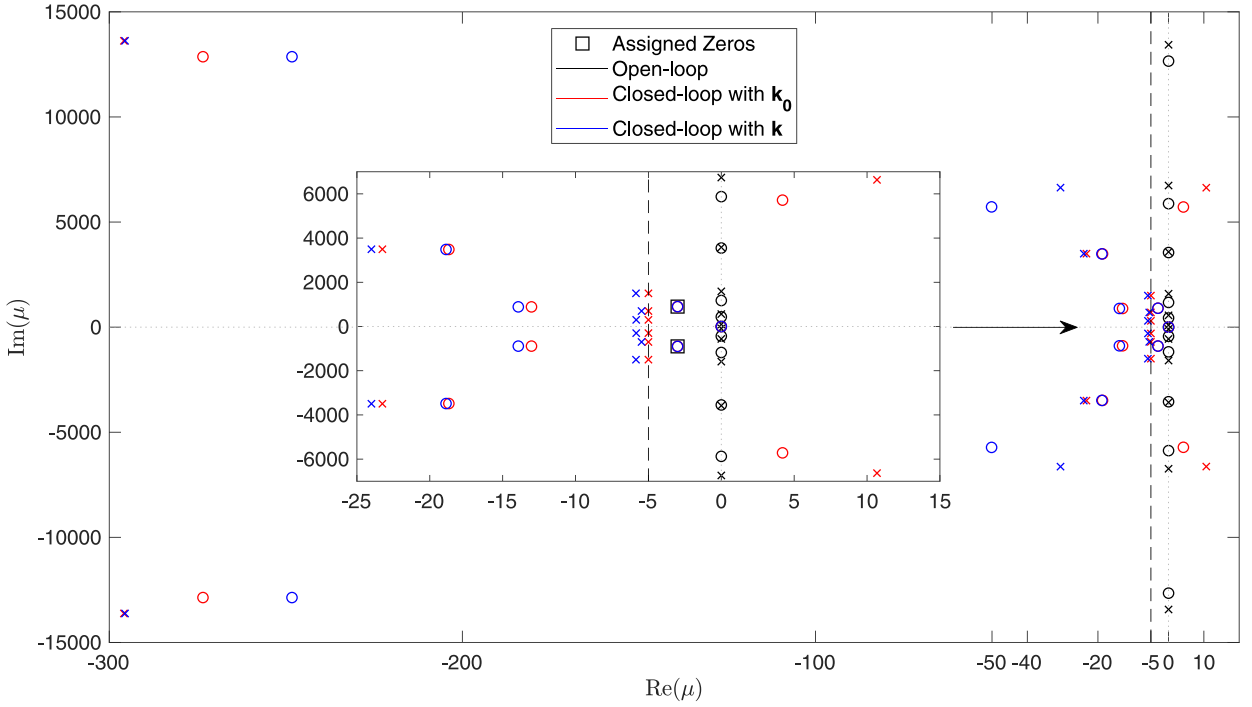

Fig. 6. Pole-zero map of $h_{33}(j\omega)$ and $\tilde{h}_{33}(j\omega)$ (test-case 3): with strategy A.

3.5. Case 4 – assignment of a pair of zeros to a cross-receptance in an asymmetric system

3.5.1. Test case description

The fourth test case exploits the asymmetric model of a slider–belt system with friction, proposed in [37–40]. This system is here adopted to show that the proposed method handles asymmetric systems too, as well as the presence of unstable (or marginally stable) poles. The system has 4-DOFs that represent the allowed translations of the three masses along the horizontal and vertical axes: $\mathbf{q} = [x_1, y_3, x_2, y_2]^{\mathbf{T}}$. The system is sketched in Fig. 8. The system matrices are reported in Eq.(42).

$$\mathbf{M} = \mathrm{diag}(m_1, m_3, m_2, m_2) \quad \mathbf{C} = \begin{bmatrix} c_1 & 0 & -c_1 & 0 \\ 0 & 0 & 0 & 0 \\ -c_1 & 0 & c_1 & 0 \\ 0 & 0 & 0 & c_0 \end{bmatrix} \quad \mathbf{b} = [0,\ 0,\ 0,\ 1]^{\mathbf{T}}$$
$$\mathbf{K_s} = \begin{bmatrix} k_1 + k_2 & 0 & -k_2 & 0 \\ 0 & k_4 + k_5 & 0 & -k_4 \\ -k_2 & 0 & k_2 + 0.5k_3 & -0.5k_3 \\ 0 & -k_4 & -0.5k_3 & k_4 + 0.5k_3 + k_c \end{bmatrix} \quad \mathbf{K_a} = \begin{bmatrix} 0 & 0 & 0 & 0 \\ 0 & 0 & 0 & 0 \\ 0 & 0 & 0 & \eta k_c \\ 0 & 0 & 0 & 0 \end{bmatrix} \tag{42}$$

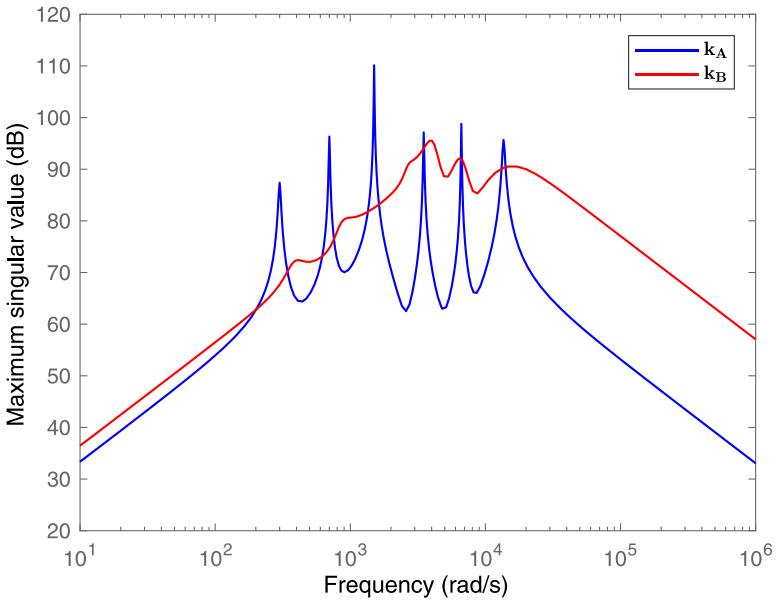

Fig. 7. Maximum singular value with $\mathbf{k_A}$ and $\mathbf{k_B}$.

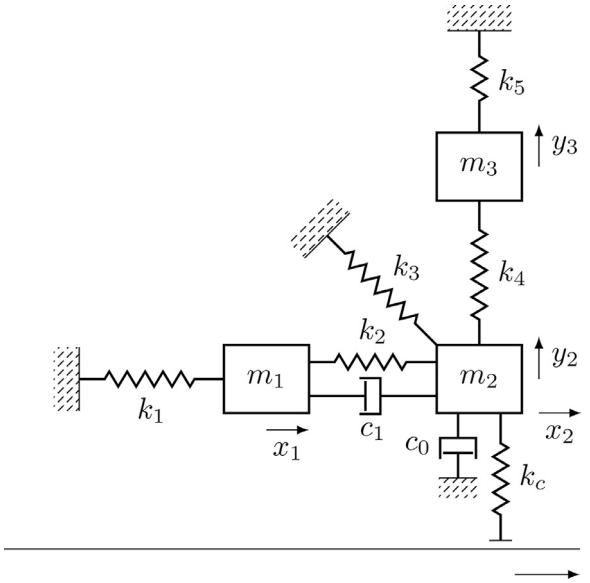

Fig. 8. Sketch of the four-DOFs slider–belt system with friction (test-case 4).

The stiffness matrix is written as the sum of two parts, $\mathbf{K} = \mathbf{K_s} + \mathbf{K_a}$. $\mathbf{K_s}$ is its symmetric part, while the asymmetric part $\mathbf{K_a}$ is due to the friction force and the pre-compression normal force acting at the slider–belt interface. The system parameters are: $m_1 = m_2 = m_3 = 1\,\text{kg}$, $k_1 = k_2 = k_3 = k_4 = k_5 = 100\,\text{Nm}^{-1}$, $k_c = 2k_1$, $c_0 = c_1 = 0.5\,\text{Nsm}^{-1}$. The friction coefficient value is assumed to be $\eta = 0.3868$. Indeed, at this point the flutter instability sets in, as stated in [38], and a pair of poles with positive real parts is obtained (i.e. $\lambda_{1,2} = 0.00 \pm \text{j}8.73$).

The assignment task consists in imposing a pair of complex conjugate zeros of the cross-receptance $h_{21}(\text{j}\omega)$ to $\mu_{1,2} = -0.5 \pm \text{j}16$ while the closed-loop poles $\lambda_1, ..., \lambda_8 \in \mathbb{C}$ are required to ensure the settling time specification defined through $\text{Re}(\lambda_i) \leq -0.25,\ i = 1, ..., 8$. The LMI region bound is shown in Fig. 8 with a dashed line. It should be noted that $h_{21}(\text{j}\omega)$ has no zeros. Hence, active control is effective to create new antiresonances in cross-receptances.

3.5.2. Method extension for systems with asymmetric stiffness matrix

The pole-zero method proposed in this paper can be applied to asymmetric systems too. Indeed, no assumption on matrix symmetry and on the stability of the open-loop system is done. The method implementation for asymmetric sys-

Table 8
Gains (test-case 4).

Stage 1: $\mathbf{k_0}$		Stage 2: $\mathbf{k} = \mathbf{k_0} + \mathbf{Vk_r}$	
$\mathbf{f_0}$	$\mathbf{g_0}$	$\mathbf{f}$	$\mathbf{g}$
−15.456	−46.194	−20.110	−42.593
2.532	84.232	3.330	75.095
−16.406	−0.299	−21.351	3.154
4.873	−23.344	5.53	7.115

tems just requires some adaptations of the equations defining the zero-assignment conditions through the receptance-based method, which is here extended in the case of rank-one control to account for the presence of asymmetric system matrices.

As shown in [39], the receptance matrix of the closed-loop system $\tilde{\mathbf{H}}(s)$ can be written in term of the receptance matrix of the open-loop system, $\mathbf{H}(s)$:

$$\tilde{\mathbf{H}}(s) = \mathbf{H}(s) - \frac{\mathbf{H}(s)\mathbf{b}(s\mathbf{f}+\mathbf{g})^{\mathbf{T}}\mathbf{H}(s)}{1+(s\mathbf{f}+\mathbf{g})^{\mathbf{T}}\mathbf{H}(s)\mathbf{b}} \tag{43}$$

In turn, the receptance matrix of the open-loop system, $\mathbf{H}(s)$, can be written in terms of the receptance matrix of the symmetric part of the open-loop system, denoted $\mathbf{H_s}(s)$, as follows:

$$\mathbf{H}(s) = (\mathbf{I} + \mathbf{H_s}(s)\mathbf{K_a})^{-1}\mathbf{H_s}(s) \tag{44}$$

where $\mathbf{H_s}(s)$ is defined as follows:

$$\mathbf{H_s}(s) = \left(s^2\mathbf{M} + s\mathbf{C} + \mathbf{K_s}\right)^{-1} \in \mathbb{C}^{N\times N} \tag{45}$$

The denominator of $\tilde{\mathbf{H}}(s)$ in Eq.(43) has been widely investigated in [38] and [39] to tackle the problem of the pole assignment. In contrast, the issue of zero-assignment, by developing its numerator, has not been considered yet in the literature. In this paper, the solution to the zero assignment through the receptance method in the case of rank-one control and full state feedback is discussed for systems with asymmetric stiffness matrix. The extension to asymmetric damping matrix is straightforward.

Let us compute once again, as proposed in Eq. (6), the *rc*-th term of the receptance matrix of the closed-loop system $\tilde{\mathbf{H}}(s)$:

$$\tilde{h}_{rc}(s) = \frac{\mathbf{e_r^T}\left[\left(1+(s\mathbf{f}+\mathbf{g})^{\mathbf{T}}\mathbf{H}(s)\mathbf{b}\right)\mathbf{H}(s) - \mathbf{H}(s)\mathbf{b}(s\mathbf{f}+\mathbf{g})^{\mathbf{T}}\mathbf{H}(s)\right]\mathbf{e_c}}{1+(s\mathbf{f}+\mathbf{g})^{\mathbf{T}}\mathbf{H}(s)\mathbf{b}} \tag{46}$$

By following some mathematical manipulations similar to those in Section 2.2, the assignment of the desired zeros of $\tilde{h}_{rc}$, μ_i, $i = 1, ..., N_z$, is performed by finding the gains $\mathbf{f}$ and $\mathbf{g}$ that solve the following linear system:

$$\begin{bmatrix} \mu_1\mathbf{t_1^T} & \mathbf{t_1^T} \\ \mu_2\mathbf{t_2^T} & \mathbf{t_2^T} \\ \vdots & \vdots \\ \mu_{N_z}\mathbf{t_{N_z}^T} & \mathbf{t_{N_z}^T} \end{bmatrix} \begin{Bmatrix} \mathbf{f} \\ \mathbf{g} \end{Bmatrix} = \begin{Bmatrix} -h_{rc}(\mu_1) \\ -h_{rc}(\mu_2) \\ \vdots \\ -h_{rc}(\mu_{N_z}) \end{Bmatrix} \tag{47}$$

where the auxiliary complex vector $\mathbf{t_i}$ in the case of asymmetric systems is defined as:

$$\mathbf{t_i} = h_{rc}(\mu_i)\mathbf{H}(\mu_i)\mathbf{b} - \left[\mathbf{e_r^T}\mathbf{H}(\mu_i)\mathbf{b}\right]\mathbf{H}(\mu_i)\mathbf{e_c} \tag{48}$$

3.5.3. Solutions

In this test case, the first stage exploits the enhanced formulation, as proposed in Eq.(14), by temporarily placing three pairs of complex conjugate poles within the desired LMI region. In particular, the same values assumed in [38] are adopted: $\lambda_{1,2} = -1 \pm \mathrm{j}9$, $\lambda_{3,4} = -1 \pm \mathrm{j}13.5$, $\lambda_{5,6} = -1 \pm \mathrm{j}18$. The concurrent pole-zero assignment for asymmetric systems can be recast in the same form of Eq.(14). The expression of $\mathbf{G_z}$ and $\mathbf{y_z}$ have been proposed in Eq.(47), while for brevity the formulation of $\mathbf{G_p}$ is omitted since it can be inferred from [39].

The solution of the determined linear system for the assignment of both the zeros and three pair of poles leads to the gain vector $\mathbf{k_0}$ reported in Table 8, while the correctness of the assignment can be inferred through Table 9. It should be noted that the unassigned pair of poles ($\lambda_{5,6} = -0.19 \pm \mathrm{j}16.66$) goes outside the LMI. Hence, the second stage is necessary.

The semidefinite optimization at the second stage has been solved with $\varepsilon_1 = \varepsilon_2 = 1\mathrm{e}-5$ and the resulting gains are reported in Table 8. The poles of the closed-loop system and the zeros of receptance $h_{21}(\mathrm{j}\omega)$ are shown in Fig. 9 and reported in Table 9: it is evident that all the pair of poles lie within the desired LMI, while no spillover on the zero occurs. Clearly, a small change on the three pre-assigned pair of poles is obtained within the feasible region, to ensure that $\lambda_{5,6}$ lie within the LMI too.

Table 9
Open-loop and closed-loop poles of the system, and zeros of receptance $h_{21}(\mathrm{j}\omega)$and $\tilde{h}_{21}(\mathrm{j}\omega)$ (test-case 4).

Open-loop zeros	Desired closed-loop zeros	Closed-loop zeros with $\mathbf{k_0}$	Closed-loop zeros with $\mathbf{k}$
	$\mu^d_{1,2} = -0.50 \pm \mathrm{j}16.00$	$\mu_{1,2} = -0.50 \pm \mathrm{j}16.00$	$\mu_{1,2} = -0.50 \pm \mathrm{j}16.00$
Open-loop poles	Desired closed-loop poles	Closed-loop poles with $\mathbf{k_0}$	Closed-loop poles with $\mathbf{k}$
$\lambda_{1,2} = 0.00 \pm \mathrm{j}8.73$	$\mathrm{Re}(\lambda_{1,2}) \leq -0.25$	$\lambda_{1,2} = -1.00 \pm \mathrm{j}9.00$	$\lambda_{1,2} = -1.22 \pm \mathrm{j}8.97$
$\lambda_{3,4} = -0.05 \pm \mathrm{j}12.19$	$\mathrm{Re}(\lambda_{3,4}) \leq -0.25$	$\lambda_{3,4} = -1.00 \pm \mathrm{j}13.50$	$\lambda_{3,4} = -0.97 \pm \mathrm{j}13.33$
$\lambda_{5,6} = -0.51 \pm \mathrm{j}16.75$	$\mathrm{Re}(\lambda_{5,6}) \leq -0.25$	$\lambda_{5,6} = -0.19 \pm \mathrm{j}16.66$	$\lambda_{5,6} = -0.26 \pm \mathrm{j}16.70$
$\lambda_{7,8} = -0.19 \pm \mathrm{j}19.86$	$\mathrm{Re}(\lambda_{7,8}) \leq -0.25$	$\lambda_{7,8} = -1.00 \pm \mathrm{j}18.00$	$\lambda_{7,8} = -1.06 \pm \mathrm{j}18.84$

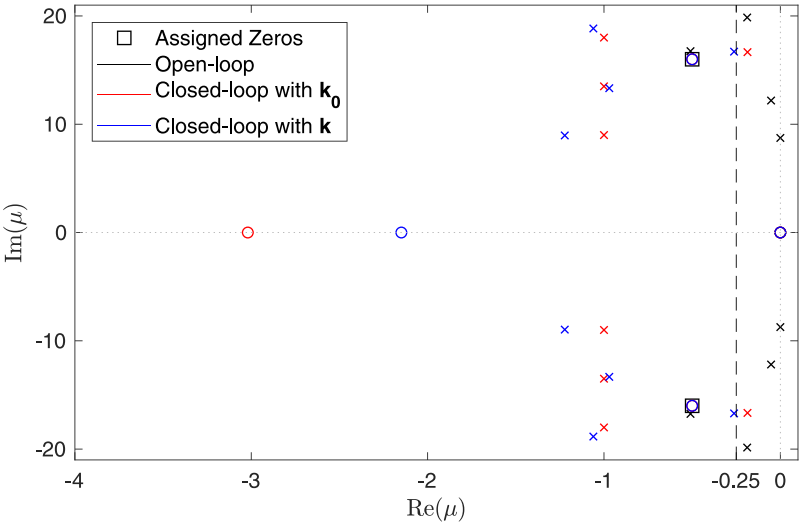

Fig. 9. Pole-zero map of $h_{21}(\mathrm{j}\omega)$ and $\tilde{h}_{21}(\mathrm{j}\omega)$ (test-case 4).

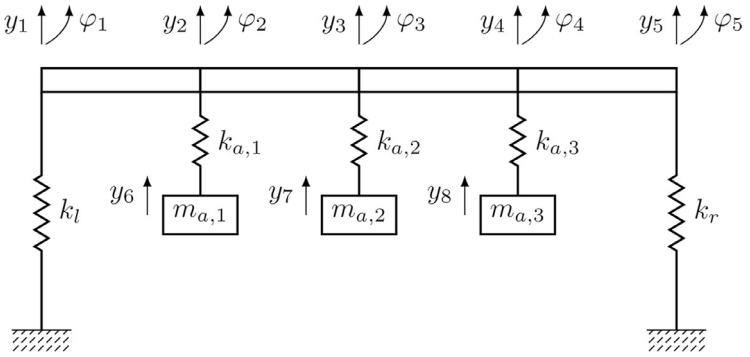

Fig. 10. Sketch of the system (test-case 5).

3.6. Case 5 – assignment of a zero to a cross-receptance in a system with lumped and distributed flexibility

The last test case exploits the simplified model similar to the one proposed in [35]. The system has 13-DOFs, that include 8 translational (y_i) and 5 rotational (φ_i) coordinates of the four Euler-Bernoulli finite elements (each one with length 0.325 m) and the three vertical translation of the suspended lumped masses: $\mathbf{q} = [y_1, \varphi_1, y_2, \varphi_2, y_3, \varphi_3, y_4, \varphi_4, y_5, \varphi_5, y_6, y_7, y_8]^{\mathbf{T}}$. The system is sketched in Fig. 10, and its parameters are: flexural rigidity $EJ = 5.1\mathrm{e}3\,\mathrm{Nm}^2$, linear mass density $\rho A = 4.97\,\mathrm{kgm}^{-1}$, $k_{a,1} = k_{a,2} = k_{a,3} = 8.7\mathrm{e}5\,\mathrm{Nm}^{-1}$, $k_l = k_r = 1\mathrm{e}3\,\mathrm{Nm}^{-1}$ and $\mathrm{m}_{a,1} = \mathrm{m}_{a,2} = \mathrm{m}_{a,3} = 25\,\mathrm{kg}$. System damping is modeled through the Rayleigh damping model: $\mathbf{C} = a\mathbf{M}+b\mathbf{K}$ with $a = 1e\text{-}2$ and $b = 1e\text{-}5$. The actuation is assumed to be described by $\mathbf{b} = [0, 0, 1, 1, 0, 0, 1, 1, 0, 0, 0, 0, 0]^{\mathbf{T}}$, to ensure the controllability of the system. The system matrices are normalized to have approximately the same order of magnitude through $\gamma = 1\mathrm{e}4$ and $\beta = 1\mathrm{e}-3$ (see Section 3.4 for the meaning of symbols). The damping matrix is scaled as $\tilde{\mathbf{C}} = \beta^{-1}\gamma^{-1}\mathbf{C}$.

Table 10
Gains (test-case 5).

Stage 1: $\mathbf{k_0}$		Stage 2: $\mathbf{k} = \mathbf{k_0} + \mathbf{Vk_r}$	
$\mathbf{f_0}$	$\mathbf{g_0}$	$\mathbf{f}$	$\mathbf{g}$
0	0	−0.879	−54,875.0
0	−14,202.3	0.118	−12,945.4
0	0	15.760	−150,550.1
−1.306	0	2.773	−7880.4
0	0	−5.166	−34,636.0
5.614	40,650.8	2.436	53,787.7
0	0	−22.254	−106,717.3
0	0	1.676	−10,119.0
0	0	7.219	39,974.9
−0.468	57.493	−1.550	−599.1
0	0	−13.413	−31,928.6
0	0	3.443	7676.0
0	0	14.273	29,054.3

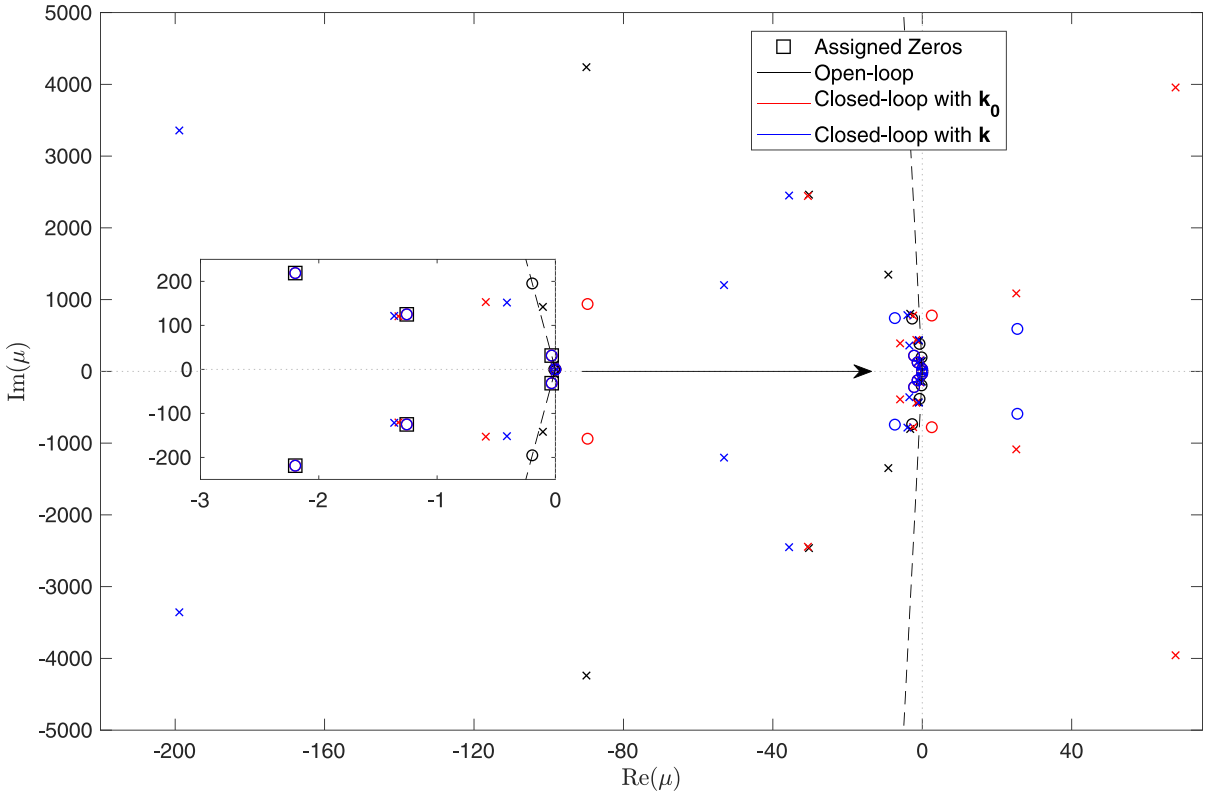

Fig. 11. Pole-zero map of $h_{19}(\mathrm{j}\omega)$ and $\tilde{h}_{19}(\mathrm{j}\omega)$, poles and zeros closest to the origin of the complex plane (test-case 5).

The assignment consists in imposing three pairs of complex conjugate zeros of $h_{19}(\mathrm{j}\omega)$, while the closed-loop poles $\lambda_1, ..., \lambda_{26} \in \mathbb{C}$ are required belong to a conic sector with magnitude 2θ such that the minimum damping of the poles is at least $\xi^{\lambda}_{\min} = 0.001$.

The complex conjugate zeros to impose are respectively: $\mu_{1,2} = -\xi_{z1}\omega_{n,z1} \pm \mathrm{j}\omega_{n,z1}\sqrt{1-\xi_{z1}}$, with $\xi_{z1} = 0.001$ and $\omega_{n,z1} = 2\pi 5\,\mathrm{rads}^{-1}$ along with $\mu_{3,4} = -\xi_{z2}\omega_{n,z2} \pm \mathrm{j}\omega_{n,z2}\sqrt{1-\xi_{z2}}$, with $\xi_{z2} = 0.01$, $\omega_{n,z2} = 2\pi 20\,\mathrm{rads}^{-1}$ and $\mu_{5,6} = -\xi_{z3}\omega_{n,z3} \pm \mathrm{j}\omega_{n,z3}\sqrt{1-\xi_{z3}}$, with $\xi_{z3} = 0.01$ and $\omega_{n,z3} = 2\pi 35\,\mathrm{rads}^{-1}$.

The resulting $\mathbf{k_0}$ that assigns the zeros in the first stage are reported in Table 10. The Semi-Definite optimization at the second stage has been solved with $\varepsilon_1 = 1\mathrm{e}-7$ and $\varepsilon_2 = 1\mathrm{e}-9$ and the obtained gains are reported in Table 10. The poles and the zeros closest to the origin are shown in Fig. 11 and reported in Table 11. The magnitude of receptance $h_{19}(\mathrm{j}\omega)$ both open-loop and closed-loop with gain $\mathbf{k}$ is shown in Fig. 12.

Table 11
Open-loop and closed-loop dominant poles of the system, and zeros of receptance $h_{19}(j\omega)$ and $\tilde{h}_{19}(j\omega)$ (test-case 5).

Open-loop zeros	Desired closed-loop zeros	Closed-loop zeros with $\mathbf{k_0}$	Closed-loop zeros with $\mathbf{k}$
$\mu_{1,2} = -0.2 \pm j195.3$	$\mu^d_{1,2} = -0.03 \pm j31.4$	$\mu_{1,2} = -0.03 \pm j31.4$	$\mu_{1,2} = -0.03 \pm j31.4$
$\mu_{3,4} = -0.7 \pm j383.1$	$\mu^d_{3,4} = -1.3 \pm j125.0$	$\mu_{3,4} = -1.3 \pm j125.0$	$\mu_{3,4} = -1.3 \pm j125.0$
$\mu_{5,6} = -2.7 \pm j735.5$	$\mu^d_{5,6} = -2.2 \pm j218.8$	$\mu_{5,6} = -2.2 \pm j218.8$	$\mu_{5,6} = -2.2 \pm j218.8$
Open-loop poles	**Desired closed-loop poles**	**Closed-loop poles with $\mathbf{k_0}$**	**Closed-loop poles with $\mathbf{k}$**
$\lambda_{1,2} = -0.005 \pm j4.9$	$\xi(\lambda_{1,2}) \geq 0.001$	$\lambda_{1,2} = -0.005 \pm j4.9$	$\lambda_{1,2} = -0.005 \pm j4.9$
$\lambda_{3,4} = -0.006 \pm j11.6$	$\xi(\lambda_{3,4}) \geq 0.001$	$\lambda_{3,4} = -1.3 \pm j120.7$	$\lambda_{3,4} = -1.4 \pm j121.4$
$\lambda_{5,6} = -0.1 \pm j141.9$	$\xi(\lambda_{5,6}) \geq 0.001$	$\lambda_{5,6} = -0.6 \pm j152.9$	$\lambda_{5,6} = -0.4 \pm j151.8$
$\lambda_{7,8} = -0.9 \pm j424.6$	$\xi(\lambda_{7,8}) \geq 0.001$	$\lambda_{7,8} = -5.9 \pm j390.7$	$\lambda_{7,8} = -3.5 \pm j360.3$
$\lambda_{9,10} = -0.9 \pm j432.7$	$\xi(\lambda_{9,10}) \geq 0.001$	$\lambda_{9,10} = -1.6 \pm j437.9$	$\lambda_{9,10} = -0.9 \pm j435.0$
$\lambda_{11,12} = -3.2 \pm j802.7$	$\xi(\lambda_{11,12}) \geq 0.001$	$\lambda_{11,12} = -2.4 \pm j777.1$	$\lambda_{11,12} = -4.0 \pm j783.8$
$\lambda_{13,14} = -9.1 \pm j1348.0$	$\xi(\lambda_{13,14}) \geq 0.001$	$\lambda_{13,14} = +25.2 \pm j1087$	$\lambda_{13,14} = -53.1 \pm j1202$
$\lambda_{15,16} = -30.3 \pm j2463$	$\xi(\lambda_{15,16}) \geq 0.001$	$\lambda_{15,16} = -30.6 \pm j2444$	$\lambda_{15,16} = -35.7 \pm j2450$
$\lambda_{17,18} = -89.9 \pm j4239$	$\xi(\lambda_{17,18}) \geq 0.001$	$\lambda_{17,18} = +67.8 \pm j3956$	$\lambda_{17,18} = -199 \pm j3357$

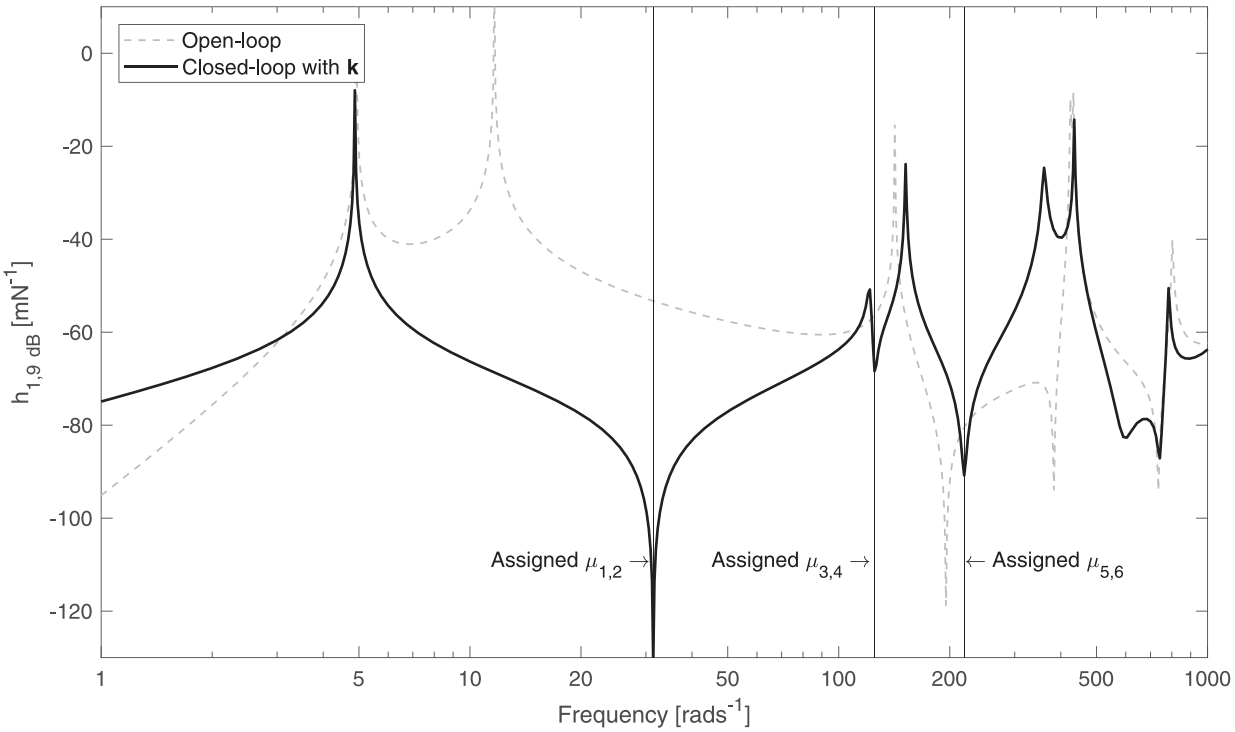

Fig. 12. Magnitude of $h_{19}(j\omega)$ before and after the modification (test-case 5).

4. Conclusions

This paper develops a full-state feedback method for active antiresonance assignment, while performing regional placement in the desired Linear Matrix Inequality (LMI) regions that set some dynamic properties such as settling time, decay rate, damping. Linear time-invariant vibrating systems are considered. The method is also extended to systems with asymmetric matrices, by proposing a more general formulation of the receptance-based zero-assignment method in the case of rank-one control.

A two-stage approach is proposed. In the first stage, that exploits the good numerical conditioning of the receptance-based formulations, the desired pairs of zeros of a prescribed closed-loop receptance are exactly assigned through the particular solution of an underdetermined linear system.

The freedom in the choice of the solution of the underdetermined system, i.e. of the gains, is the leverage of the second stage of the method that uses a first-order formulation of the model to take advantage of the powerful theory of LMI. In this stage, an additive gain correction is computed by solving the homogeneous system related to the zero-assignment problem, thus ensuring that such a correction does not cause spillover on the assigned zeros. The goal of this term is to assign all the closed-loop poles within the region of the complex plane that ensures the desired response. Since the pole assignment

problem with the no-spillover condition leads to a Bilinear Matrix Inequality, a change of variables has been exploited to cast the problem as a standard LMI. The regional pole assignment problem is finally recast as a semidefinite optimization and a solution that reduces the control effort is calculated.

A great advantage of this approach is that it enlarges the performances of the state-of-the-art active control approaches to antiresonance assignment that usually neglect the spillover on the poles, that might cause slow and undamped transient response and instability too. A second advantage is related to the use of LMI, that easily allows imposing the desired properties through shifted half planes, strips, ellipses, disks, conic sectors, as well as any intersection of the above regions of the complex plane. Finally, the availability of interior-point optimization algorithms, together with some numerical tools here suggested for improving the solution (such as the model matrix scaling, and the use of strict inequalities in the SDP), enables the use of the method for several systems.

Numerical validation is provided in five different test cases, also taken among the existing literature, which include a meaningful set of samples where the method can be applied. The five examples refer to the case of rank-one control, which is the one where the use of receptance approach is more straightforward due to a simple formulation of the zero-assignment problem. Nonetheless, the proposed idea of the two-stage approach can be extended to higher-rank control by exploiting suitable methods for gain computing in the first step. In all the test cases, the exact placement of the desired zeros in the desired locations together with the clustering of all the poles within the desired regions prove the correctness and the effectiveness of the proposed approach.

CRediT authorship contribution statement

Dario Richiedei: conceptualization, theoretical development, formal analysis, verification of the results and writing of the paper.

Iacopo Tamellin: conceptualization, theoretical development, formal analysis, software development, verification of the results and writing of the paper.

Declaration of Competing Interest

The authors declare that they have no known competing financial interests or personal relationships that could have appeared to influence the work reported in this paper.

Acknowledgment

The second author acknowledges the financial support of the Cariparo foundation (“Fondazione Cassa di Risparmio di Padova e Rovigo”) through a Ph.D. scholarship.

References

[1] H. Frahm, Device for damping vibrations of bodies, U.S. Pat. (1911) https://doi.org/989-95.
[2] Y.M. Ram, S. Elhay, The theory of a multi-degree-of-freedom dynamic absorber, J. Sound Vib. 195 (1996) 607–615, doi:10.1006/jsvi.1996.0449.
[3] D. Richiedei, I. Tamellin, A. Trevisani, A general approach for antiresonance assignment in undamped vibrating systems exploiting auxiliary systems, Mech. Mach. Sci. (2019), doi:10.1007/978-3-030-20131-9_407.
[4] J.E. Mottershead, Structural modification for the assignment of zeros using measured receptances, J. Appl. Mech. Trans. ASME. 68 (2001) 791–798, doi:10.1115/1.1388616.
[5] J.E. Mottershead, Y.M. Ram, Inverse eigenvalue problems in vibration absorption: passive modification and active control, Mech. Syst. Signal Process. 20 (2006) 5–44, doi:10.1016/j.ymssp.2005.05.006.
[6] S.H. Tsai, H. Ouyang, J.Y. Chang, Inverse structural modifications of a geared rotor-bearing system for frequency assignment using measured receptances, Mech. Syst. Signal Process. 110 (2018) 59–72, doi:10.1016/j.ymssp.2018.03.008.
[7] R. Belotti, D. Richiedei, I. Tamellin, Antiresonance assignment in point and cross receptances for undamped vibrating systems, J. Mech. Des. 142 (2019) 022301, doi:10.1115/1.4044329.
[8] D. Richiedei, I. Tamellin, A. Trevisani, Simultaneous assignment of resonances and antiresonances in vibrating systems through inverse dynamic structural modification, J. Sound Vib. 485 (2020) 115552, doi:10.1016/j.jsv.2020.115552.
[9] Y.M. Ram, Pole-zero assignment of vibratory systems by state feedback control, JVC/J. Vib. Control. 4 (1998) 145–165, doi:10.1177/107754639800400204.
[10] Y.M. Ram, J.E. Mottershead, Receptance method in active vibration control, AIAA J. 45 (2007) 562–567, doi:10.2514/1.24349.
[11] J.E. Mottershead, M.G. Tehrani, S. James, Y.M. Ram, Active vibration suppression by pole-zero placement using measured receptances, J. Sound Vib. 311 (2008) 1391–1408, doi:10.1016/j.jsv.2007.10.024.
[12] K.V. Singh, B.N. Datta, M. Tyagi, Zero assignment in vibration: with and without time delay, in: 2007 Proc. ASME Int. Des. Eng. Tech. Conf. Comput. Inf. Eng. Conf. DETC2007, 2008, doi:10.1115/DETC2007-34819.
[13] K.V. Singh, B.N. Datta, M. Tyagi, Closed form control gains for zero assignment in the time delayed system, J. Comput. Nonlinear Dyn. 6 (2011) 021002, doi:10.1115/1.4002340.
[14] G. Cazzulani, F. Resta, F. Ripamonti, Active modal tuned mass damper for smart structures, Eng. Lett. 19 (2011) 1–10.
[15] S. Cinquemani, F. Braghin, F. Resta, Act. Passiv. Smart Struct. Integr. Syst, 2017, p. 2017, doi:10.1117/12.2259987.
[16] B. Boudon, F. Malburet, J.C. Carmona, Bond graph modeling and simulation of a vibration absorber system in helicopters, Bond Graphs Model. Control Fault Diagnosis Eng. Syst. Second Ed, 2016, doi:10.1007/978-3-319-47434-2_11.
[17] B. Boudon, F. Malburet, J.C. Carmona, Simulation of a helicopter’s main gearbox semiactive suspension with bond graphs, Multibody Syst. Dyn. 40 (2017) 375–405, doi:10.1007/s11044-016-9536-5.
[18] R. Belotti, D. Richiedei, Pole assignment in vibrating systems with time delay: an approach embedding an a-priori stability condition based on Linear Matrix Inequality, Mech. Syst. Signal Process. 137 (2020) 106396, doi:10.1016/j.ymssp.2019.106396.

[19] R. Belotti, D. Richiedei, I. Tamellin, Pole assignment for active vibration control of linear vibrating systems through linear matrix inequalities, Appl. Sci. 10 (2020) 5494, doi:10.3390/app10165494.
[20] M. Chilali, P. Gahinet, H∞ design with pole placement constraints: an LMI approach, IEEE Trans. Automat. Contr. 41 (1996) 358–367, doi:10.1109/9.486637.
[21] M. Chilali, P. Gahinet, P. Apkarian, Robust pole placement in LMI regions, IEEE Trans. Automat. Contr. 44 (1999) 2257–2270, doi:10.1109/9.811208.
[22] D. Henrion, M. Šebek, V. Kucera, Robust pole placement for second-order systems: an LMI approach, IFAC Proc. (2003) 419–424 Vol., doi:10.1016/S1474-6670(17)35700-2.
[23] D. Henrion, M. Šebek, V. Kučera, V. Kucera, Robust pole placement for second-order systems: an LMI approach, Kybernetika 41 (2005) 1–14, doi:10.1016/S1474-6670(17)35700-2.
[24] Z. Li, J. Lam, Multiobjective controller synthesis via eigenstructure assignment with state feedback, Int. J. Syst. Sci. (2016), doi:10.1080/00207721.2015.1112444.
[25] F.A. Faria, E. Assunção, M.C.M. Teixeira, R. Cardim, N.A.P. Da Silva, Robust state-derivative pole placement LMI-based designs for linear systems, Int. J. Control. (2009), doi:10.1080/00207170801942188.
[26] H.K. Tam, J. Lam, Robust deadbeat pole assignment with gain constraints: an LMI optimization approach, Optim. Control Appl. Methods. (2000), doi:10.1002/oca.676.
[27] M.O. de Almeida, J.M. Araújo, Partial Eigenvalue Assignment for LTI Systems with D -Stability and LMI, J. Control. Autom. Electr. Syst. 30 (2019) 301–310, doi:10.1007/s40313-019-00457-y.
[28] S. Xu, J. Lam, A survey of linear matrix inequality techniques in stability analysis of delay systems, Int. J. Syst. Sci. (2008), doi:10.1080/00207720802300370.
[29] Y.M. Ram, S. Elhay, Pole assignment in vibratory systems by multi-input control, J. Sound Vib. (2000), doi:10.1006/jsvi.1999.2622.
[30] D. Peaucelle, D. Arzelier, O. Bachelier, J. Bernussou, A new robust script D sign-stability condition for real convex polytopic uncertainty, Syst. Control Lett. (2000), doi:10.1016/S0167-6911(99)00119-X.
[31] K. Chen, Matrix preconditioning techniques and applications, Cambridge University Press, Cambridge, UK, 2005.
[32] J. Löfberg, YALMIP: a toolbox for modeling and optimization in MATLAB, in: Proc. IEEE Int. Symp. Comput. Control Syst. Des., 2004, doi:10.1109/cacsd.2004.1393890.
[33] J. Fiala, M. Kočvara, M. Stingl, PENLAB: a MATLAB solver for nonlinear semidefinite optimization, ArXiv (2013) 5240.
[34] Z. Liu, W. Li, H. Ouyang, D. Wang, Eigenstructure assignment in vibrating systems based on receptances, Arch. Appl. Mech. 85 (2015) 713–724, doi:10.1007/s00419-015-0983-x.
[35] R. Belotti, D. Richiedei, A. Trevisani, Optimal design of vibrating systems through partial eigenstructure assignment, J. Mech. Des. Trans. ASME. 138 (2016) 071402, doi:10.1115/1.4033505.
[36] H. Ouyang, D. Richiedei, A. Trevisani, Pole assignment for control of flexible link mechanisms, J. Sound Vib. (2013), doi:10.1016/j.jsv.2013.01.004.
[37] H. Ouyang, Pole assignment of friction-induced vibration for stabilisation through state-feedback control, J. Sound Vib. 329 (2010) 1985–1991, doi:10.1016/j.jsv.2009.12.027.
[38] H. Ouyang, A hybrid control approach for pole assignment to second-order asymmetric systems, Mech. Syst. Signal Process. 25 (2011) 123–132, doi:10.1016/j.ymssp.2010.07.020.
[39] M.G. Tehrani, H. Ouyang, Receptance-based partial pole assignment for asymmetric systems using state-feedback, Shock Vib. 19 (2012) 564061, doi:10.1155/2012/564061.
[40] Y. Liang, H. Yamaura, H. Ouyang, Active assignment of eigenvalues and eigen-sensitivities for robust stabilization of friction-induced vibration, Mech. Syst. Signal Process. 90 (2017) 254–267, doi:10.1016/j.ymssp.2016.12.011.